STOCHASTIC PROGRAMMING MODELS: COMMUNITY HEALTH PATHWAYS SCHEDULING AND OPTIMAL VACCINE ALLOCATION

A Dissertation

by

JIANGYUE GONG

Submitted to the Graduate and Professional School of
Texas A&M University
in partial fulfillment of the requirements for the degree of

DOCTOR OF PHILOSOPHY

Chair of Committee,	Lewis Ntaimo
Committee Members,	Amarnath Banerjee Mark Lawley Ali Mostafavidarani
Head of Department,	Lewis Ntaimo

May 2022

Major Subject: Industrial Engineering

ABSTRACT

The World Health Organization (WHO) designated the novel COrona VIrus (COVID-19) a global pandemic. This pandemic combined with the growing and aging population has created a crisis of unprecedented dimension regarding shortages in health care workforce. COVID-19 has exacerbated care coordination by pushing the healthcare system to a limit in terms of rationing the allocation of scarce and valuable social and medical resources. Therefore, in this dissertation, we consider a Community Health Pathways HUB model to optimize resource scheduling and optimal vaccination allocation models to control the outbreaks.

Scheduling pathways involves uncertainty in resource availability because as human resources may not report for work due to unforeseen circumstances such as delays in previous assignments. Similarly, the vaccination allocation problem involves uncertainty in COVID-19 characteristics, such as vaccine efficacy towards mutating variants, infectivity, and susceptibility. Stochastic programming is a framework for modeling optimization problems that involve data uncertainty. This dissertation considers three fundamental approaches of stochastic programming: 1) stochastic programming with recourse in which infeasibility is not allowed, only recourse/corrective actions with a certain cost; 2) chance-constrained programming in which infeasibility is allowed up to a certain probability; and 3) integrated chance-constrained programs that not only allow for infeasibility but also restrict it up to a certain threshold. The first approach is applied to a community health pathways scheduling problem, while the last two approaches are applied to optimal vaccine allocation under uncertainty for COVID-19.

DEDICATION

I would like to dedicate this work to my parents, my family and my friends who are my strong supporters and believers to achieve this accomplishment. Without their love and encouragement, I would not have been where I am today and who I am today.

ACKNOWLEDGMENTS

I would like to express my sincere gratitude to my advisor, Dr. Lewis Ntaimo, for his guidance, inspiration and suggestions for developing this dissertation and for his support and mentorship throughout the journey towards this degree. He gave me all the freedom to pursue my research, while ensuring that I stay on course and do not deviate from the core of my research. Without his able guidance, compiling this dissertation would not have been possible and I shall be eternally grateful to him for his assistance. I would like to thank Dr. Amarnath Banerjee, Dr. Mark Lawley, and Dr. Ali Mostafavidarani for agreeing to serve on my committee. Finally, I would like to acknowledge the Department of Industrial & Systems Engineering at Texas A&M University for providing all the necessary assistance and resources I need to successfully conduct my research.

CONTRIBUTORS AND FUNDING SOURCES

Contributors

This work was supported by a dissertation committee consisting of Professor Lewis Ntaimo [advisor], Amarnath Banerjee, Mark Lawley of the Department of Industrial and Systems Engineering and Professor Ali Mostafavidarani of the Department of Civil Engineering.

The data analyzed for Chapter 5 was partially provided by Krishina Gujjula. All other work conducted for the dissertation was completed by the Jiangyue Gong independently.

Funding Sources

There are no outside funding contributions to acknowledge related to the research and compilation of this document.

NOMENCLATURE

WHO	World Health Organization
COVID-19	COronaVIrus Disease of 2019
CHPs	Community Health Pathways
SP	Stochastic Programming
CC	Chance-Constrained
ICC	Integrated Chance-Constrained
SAA	Sample Average Approximation
DEP	Deterministic Equivalent Programs
MIP	Mixed Integer Program
SMIP	Stochastic Mixed Integer Program
ACS	Acute Coronary Syndrome
ASM	Asthma
BHI	Behavioral Health Intervention
CAT	Care Team
CCA	Companion or Care Attendant
CHI	Closed Head Injury
CSB	Caesarean Birth
DMV	Domestic Violence
DNC	Dietitian and Nutrition Consultant
DPC	Dying Person Care
FDI	Food Insecurity
HUS	Housing

INS	Insurance
MDH	Medical Home
MDR	Medical Referral
PTS	Prime Time Sister Circle
SMC	Smoking Cessation
SSR	Social Service Referral
TBS	Thrombolysis
TRH	Transportation-HEZ
PNt	Patient Navigator
EDU	Educator
LAS	Liaison
OTW	Outreach Worker
PEC	Patient Counselor
HIP	Health Interpreter
TRL	Training Location
CHA	Community Health Advisor
TRS	Transporter
WB	Workload Balancing
NWB	No Workload Balancing
CV	Coefficient of Variation
$\mathcal{B}$	Bernoulli Distribution
$\mathcal{U}$	Uniform Distribution

TABLE OF CONTENTS

Page

LIST OF FIGURES

FIGURE Page

LIST OF TABLES

TABLE Page

1. INTRODUCTION AND MOTIVATION

This dissertation focuses on mathematical optimization models and solutions for health care related applications involving uncertain parameters. Two important problems are investigated, one from healthcare and the other from epidemiology. Specifically, we address: 1) community health pathways modeling and scheduling under uncertainty in resource availability, and 2) optimal COVID-19 vaccination allocation under uncertainty in transmission characteristics.

1.1 Motivation

The motivation of this dissertation comes from the increasing demand in health care workforce and lack of coordination in health care system. High cost and disconnected administration are two of the main characteristics of the U.S. healthcare system [1]. Inadequate care coordination is a key contributor to annul healthcare cost due to avoidable complications and unnecessary, ineffective, and wasteful services [2]. The U.S. healthcare system is still undergoing the needed transformation that aims to achieve the dual goals of cost-effective delivery and improved patient outcomes. At the core of this transformation is an emphasis on encouraging physicians, hospitals, and other healthcare stakeholders to work more closely to better coordinate patient care through integrated goals and data sharing [3]. Performing care coordination involving disparate resources presents significant challenges in terms of scheduling, adhering to the care activities protocols, and tracking the progress of these activities for each patient in the system.

In March of 2020, the World Health Organization (WHO) designated the novel **CO**rona**VI**rus (COVID-19) a global pandemic. This virus causes a series of respiratory illnesses and has spread globally with millions of confirmed cases and deaths. The pandemic combined with the growing and aging population has created a healthcare crisis of unprecedented dimension regarding shortages in resources, such as nurses, physicians, community health workers and other health related professionals. Individuals with complex health needs and chronic health conditions have a higher risk of having severe conditions if they contract COVID-19. Addressing these complex needs

requires a combination of multiple services and support from a wide variety of resources at different levels of the healthcare system. COVID-19 has exacerbated care coordination by pushing the healthcare system to a limit in terms of rationing the allocation of scarce and valuable social and medical resources.

Scheduling and coordinating constrained resources in community healthcare settings at a centralized community level can be challenging due to limited resources and inherent dynamics of the processes and the organizational structures. In this work, we adopt the Community Health Pathways (CHPs) HUB model. This model provides a delivery system for care coordination services in a community setting with a goal of improving health outcomes for the high-risk individuals and provide preventive care [4]. In this HUB model, CHPs are a standardized tool that details multiple steps of a healthcare-related service and the required resources for each step.

We derive a mathematical model for optimally scheduling pathways under uncertainty in resource availability. We devise a simulation model of a Pathways Community HUB to schedule patients over a period of time. Both models were implemented and applied to data for a real Pathways Community HUB of a U.S. county involving multiple CHPs and limited resources. The computational study shows that patient wait time depends on the HUB resources' uncertain availability and patient demand, with high demand resulting in longer waiting time. The study also shows that workload balancing is beneficial in terms of providing schedules with similar workloads across community health workers while providing waiting times that are comparable to the results with no workload balancing. Several managerial insights are obtained, including the recommendation to managers to use workload balancing not only to minimize patient waiting time, but also to guarantee patient schedules that result in equitable use of the limited HUB resources.

The COVID-19 pandemic has exerted great pressure on scarce medical resources. Without an accurate cure for COVID-19, vaccination is the key to control the outbreaks. In the U.S., at the time of writing this dissertation, three vaccines are authorized and recommended: Pfizer-BioNTech, Moderna, and Johnson & Johnson's Janssen. As of November, more than half of the population in the U.S. were fully vaccinated against COVID-19. However, SARS-Cov-2 transmission is still

at high levels in different regions of the U.S. Just like the other virus, the SARS-CoV-2 virus keeps changing through mutation. Evidence shows that some of the new variants, such as the currently circulating Alpha, Delta and Gamma variant, can be more severe in terms of illness and transmissibility, and the vaccine may be less efficacious [5, 6] compared to its ancestor variant. There is an urgent need for an effective vaccination strategy to be implemented to compete with the variant mutation and fading vaccine efficacy.

An effective vaccination allocation strategy is sensitive to the essential and conclusive epidemiological characteristics of the virus, vaccine efficacy, vaccine-induced, and natural immunity. In addition, household is a significant contributor and high risk setting for COVID-19 transmission, and a critical factor in community spread. The recent variants have a relatively high transmission rate within household. If a member in a household is infected, the other members who live in the same household are more likely to be infected. For those who reside in larger household sizes, if one of them is infected, there are more members to spread the disease to than those who reside in smaller households. To guarantee maximum effectiveness with limited supply, a method that can capture parameter uncertainty and demographic variability is needed. Therefore, in this dissertation, we derive mathematical models to account for the uncertainty in parameters for effective vaccination allocation in communities. In this dissertation, a vaccination policy prescribes the minimum proportion of population to vaccinate in a community.

Scheduling community pathway involves uncertainty in resource availability because as human resources may not report for work due to unforeseen circumstances such as delays in previous assignments. Similarly, vaccination allocation problem involves uncertainty in COVID-19 characteristics, such as vaccine efficacy towards mutating variants, infectivity, and susceptibility. Stochastic programming (SP) is a framework for modeling optimization problems that involve data uncertainty. Random variables are used to model uncertainty in parameters. When the parameters are uncertain, one might seek a solution that is feasible for all realizations of the random parameters over a given objective function or a solution that accepts a certain level of *infeasibility*. This dissertation considers three fundamental approaches of SP: 1) SP with recourse in which infeasibility is

not allowed, only recourse/corrective actions with a certain cost [7, 8]; 2) chance-constrained (CC) programming in which infeasibility is allowed [9]; and 3) integrated chance-constrained programs (ICC) that not only allows for infeasibility but also restricts it up to a certain threshold [10, 11]. The first approach is applied to a community health pathways scheduling problem, while the last two approaches are applied to optimal vaccine allocation under uncertainty for COVID-19.

In the CC approach, infeasibility is accepted up to a specified level, but the amount by which the constraints are violated is not considered. This approach is applied to a wide range of applications by practitioners who prefer a qualitative risk measure. However, the feasible set defined by CC is generally non-convex. Furthermore, the reformulation of CC is a mixed-integer program, which is also difficult to solve. The mathematical properties of CC motivated researchers to consider alternatives that accept infeasibility. In 1986, Haneveld introduced ICC to allow for constraint violation while bounding the amount of violation [10].

In cases where constraint violation is critical to the application, ICC might be more appropriate since it bounds the amount of violation. In this approach, the constraint violation either above or below the target is bounded, but not both. A target could be a desired outcome. For instance, in the optimal vaccination allocation problem the target is one. The goal is to drive post-vaccination reproduction number to be below one. In practice, constraint violation above and below a target may be critical for decision making. Therefore, in this dissertation we also consider an extension of the ICC model for this case. We derive a deterministic equivalent program for solving two-sided ICC problems. For instances with a large number of scenarios, we consider a reduced form algorithm based on [11] that adds cuts iteratively to reach the optimal solution.

1.2 Research Contribution

This dissertation makes contributions to the literature on stochastic programming and applications in two main areas: 1) a stochastic programming model for community health pathways scheduling under uncertainty in resource availability. A simulation model of a generic Pathways Community HUB is devised and implemented to evaluate CHPs schedules determined by optimization model; and 2) new CC and ICC models for optimally allocating vaccines in multiple

communities under uncertainty in transmission characteristics and a computational study based on real data.

1.2.1 Community Health Pathways Modeling and Scheduling

Under this contribution, a two-stage SP model is derived to handle CHPs scheduling involving uncertainty in resource availability. To the best of our knowledge, this the first SP with workload balancing for pathway scheduling under uncertainty to minimize patient waiting time. We also devise and implement a computer simulation for a Pathways Community HUB. This simulation model allows modeling and simulating arrivals of pathway requests, booking available resources based on the optimal solution provided by the model, and updating resource availability. In addition, this model-based approach allows for progress tracking and notification for individual CHPs and allows to compute and monitor performance over time.

1.2.2 Optimal COVID-19 Vaccination Allocation

We introduce a new stochastic programming based model to determine optimal vaccination policies to control epidemics and apply it to COVID-19. This new model considers randomness in parameters, including human interactions, COVID-19 transmission characteristics, and vaccine efficacy towards different emerging COVID-19 variants. The model captures the socio-demographic variations in population's household types and individual vaccination status. An optimal vaccination policy provides the minimum number of vaccinations required to control outbreaks at pre-determined reliability levels. We perform several case studies to test the new model on a set of neighboring counties in the U.S. state of Texas to generate optimal vaccination allocation strategies with homogeneity in population. Results obtained from our model can provide an evidence-based rationale for health authorities to make critical decisions.

The rest of this dissertation is organized as follows: Chapter 2 reviews closely related literature on stochastic programming with recourse, CC, ICC, community health pathways and vaccine allocation. The fundamental concepts of stochastic programming models and extension of CC to ICC model are presented in Chapter 3, along with a reduced form algorithm to efficiently solve ICC

instances with a large number of scenarios. The SP model and computer simulation for community health pathways scheduling under uncertainty in resource availability are presented in Chapter 4. Chapter 5 develops an ICC model with a set of reliability levels to optimally allocate vaccines under application to optimal vaccine allocation under uncertainty in COVID-19 characteristics. Finally, concluding remarks and future research are given in Chapter 6.

2. LITERATURE REVIEW

2.1 Stochastic Programming

In this chapter, we present literature on stochastic programming, pathways and vaccine allocations. Stochastic programming is an approach for modeling optimization problems that involve uncertainty. There are two well-known approaches on stochastic programming regarding infeasibility. One approach is to penalize the effects of infeasibility, whereas the other one is to restrict infeasibility. In the case where infeasibility is accepted, CC and ICC are introduced. With CC, infeasibility is accepted, but only with a specified probability, whereas ICC accepts infeasibility at a certain cost. The other approach where infeasibility is restricted leads to the models so called two-stage stochastic programming with recourse. In stochastic programming with recourse, infeasibility is not accepted, but corrective actions are taken afterwards with a certain penalty. This approach gives a foundation of the proposed work on two-sided ICC.

The major historical developments of stochastic programming is presented in Section 2.1.1. For CC and ICC, the literature is presented in Section 2.1.2. The stochastic programming with recourse approach is applied to a community health pathways scheduling problem and the literature on pathways and pathways scheduling are discussed in Section 2.2. CC and ICC are applied to optimal vaccine allocation under uncertainty, with a focus on COVID-19 and related literature for this topic is presented in Section 2.3.

Several papers have studied the relation between CC, ICC and stochastic programming with recourse, and established certain equivalences among these modeling techniques [10, 12, 13]. However, the mathematical equivalence does not mean that they can be simply exchanged. In CC, risk is measured qualitatively, and the probability of infeasibility is permitted up to a specified level. However, the amounts by how much the constraints are violated are not taken into account. In the case when constraints represent quantitative goals instead of technical or logical necessities, ICC might be applied to accept a high probability of infeasibility if the constraints are violated by a

relatively small amount. In ICC, we can impose an upper bound on the expected violation amount. Unlike ICC, in recourse models, infeasibility is not accepted, the corrective actions are required afterwards with a certain cost. Depending on the circumstances, some practical applications, the specification of infeasibility costs might be more appropriate than a specification of a feasibility probability level, or vice versa. For example, if the application is willing to take recourse actions with some cost, stochastic programming with recourse can be applied. If the application is willing to accept infeasibility, CC or ICC approach is more suitable.

If the decisions have to be made before or at least without knowledge of any realization of the random parameters, we call this *here-and-now* decision making. For example, in CC and ICC, without knowing any further information on the realization of the random parameters, all the decisions are made at the moment. In the case where decision makers are able to wait for the realization of the random parameters, this is *wait-and-see* decision making. For example, the stochastic programming with recourse, the first-stage decisions are made here-and-now without full information of the uncertain parameters, and the second-stage decisions are made based both on the first-stage decisions and the realization of the random parameters.

2.1.1 Stochastic Programming with Recourse

Two-stage stochastic programming with recourse was introduced by Dantzig in 1955 [13]. The first-stage decisions are the ones that are determined now; decisions in the second-stage depend on both the uncertainty and the first-stage decisions. Since then, numerous studies have sought to develop decomposition methods to solve stochastic programs. As the number of scenarios increases, there is an increasing chance for the stochastic program to become computationally intractable. In 1961, Dantzig and Wolfe established the Dantzig-Wolfe decomposition (DWD) approach of linear programming, in particular those with a special block-angular structure [14, 15]. This block-angular structure often arise in applications where the system is coupled with subsystems.

A classic decomposition dealing with block-diagonal structure was originally introduced by Benders in 1962 [16]. Before Benders' method was developed, this block-diagonal structure problem had to be solved using deterministic equivalent problem, which is computational very expen-

sive for large instances. Benders partitioned the block-diagonal structures into master problem and subproblem. However, the subproblem created by Bender's method is still dense with instances that have large scenario size. Since Benders decomposition only returns one cut to the master problem in each iteration, the convergency can be slow for some computationally demanding problems [17].

Slyke proposed L-shaped method to solve two-stage linear recourse models to accelerate the convergence rate. The L-shaped method separates the large subproblem into many smaller subproblems [18]. At each iteration, the first-stage solutions are passed to the second-stage, and the second-stage subproblems are solved with the first-stage decisions given. Then the appropriate optimality or feasibility cuts are added to the master problem based on the solutions generated from the subproblems.

To address the computational challenge for dealing large-scale instances, decomposition methods have been proposed to solve two-stage stochastic programs, including stochastic decomposition [19], subgradient decomposition [20] and disjunctive decomposition [21]. However, the number of subproblems is associated with the number of scenarios, and the model size increases exponentially as the number of scenarios increases. These methods can sometimes still be computationally demanding. Shapiro et al. suggested Sample Average Approximation (SAA) algorithm that uses a computer simulation-based approach [22]. The subporblems are generated by randomly sampling some scenarios. The expected objective function is approximated by a sample average estimate derived form a random sample. The process is repeated with different samples to obtain candidate solutions.

2.1.2 Chance-constrained and Integrated Chance-constrained programming

Chance-constrained programming was introduced in 1959 by Charnes and Cooper [23], and established the deterministic equivalent programs (DEP) for CC with constant constraint matrix [24]. A few years later, Karaoka extended the CC with uncertainty in the A matrix [25]. Prékopa developed joint chance-constrained programs and proposed DEP under certain assumptions on the distribution of the random right-hand side [26]. In CC approach, infeasibility is accepted up

to a certain probability, and it is appealing to some practitioners who prefer to use a qualitative risk measure. However, it is well known that CC is non-convex when the uncertainty parameters follow a discrete distribution [27, 28]. Non-convexity brings great computational difficulties, and if chance constraints are applied as risk constraints, they can only be handled computationally using discrete distributions. Furthermore, reformulation of CC results in a mixed-integer program, which is also difficult to solve in general. For linear constraints and finite discrete distribution, cutting plane approach is available for mixed-integer reformulations [29, 30]. For a small or moderate size problem, we can use the current available mix-integer program solver to solve, however, the problem involves big-M generally have a weak LP-relaxation. The mathematical properties of CC motivate alternative models that accept infeasibility.

In 1986, Haneveld proposed ICC [10] that captures risk quantitatively by accepting infeasibility with a certain cost. The studies on ICC are limited. Haneveld et al. proposed a reduced form algorithm that can efficiently solve ICC with discretely distributed random vector by generating optimality cuts [11], and the other closely related work they have done is multistage ICC model and conducted a computational study using dynamic stochastic programming approach [31].

2.2 Community Health Pathways Scheduling

Community healthcare agencies in the U.S. are tasked with providing medical, behavioral, and social services to the individuals in need. With limited resources, providing such services requires careful coordination. Care coordination is the organization of care activities among individual clients and providers to facilitate the appropriate delivery of healthcare services [32]. Community care coordination works at the community level to improve the quality of care for individuals by coordinating community-based health and social services. These community-based services have been shown to play a vital role in addressing some of the nation's most challenging health problems, including health disparities and the rising chronic health conditions such as obesity and diabetes [33]. Addressing these complex needs requires a combination of multiple services (medical services, behavioral health services, and social services) and support from a wide variety of community-based resources in order to reduce the health and social barriers to improve healthcare

outcomes [34]. This complexity poses significant challenges in terms of effectively connecting the different parties (clients, agencies, service providers) and coordinating them to work in concert to achieve positive outcomes.

Performing care coordination involving disparate resources can be challenging in terms of scheduling and adhering to the care activities protocols. In this dissertation, we focus on community care coordination using Pathways Community HUB model of care coordination. The pathway model of care coordination is a construct that was introduced to enable coordination of care activities of different organizations and their services by focusing on the progress and outcomes of individual clients as they traverse the care organizations [35]. In turn, pathways coordination can enable a comprehensive approach to community health service focused on reducing the healthcare inequalities to improve health outcomes for the community.

In healthcare settings like hospitals, care coordination involves coordinating with all of the different service providers to facilitate the patient's interactions with the healthcare system to improve their health outcomes. The service process involves various interfaces and accurate information is critical for healthcare practitioners to make both quick and right decisions. However, the information sometimes gets lost or mistaken while passing through the service delivery. The lack of care coordination leads to inferior outcomes for patients. For instance, unnecessary or repetitive diagnostic tests, unnecessary emergency room visits, and preventable hospital admissions and readmissions all lead to lower quality of care and ultimately, worse health outcomes. Clinical or care pathways (treatment protocols), as they are often referred to in clinical settings, can alleviate such issues. Studies have shown that clinical pathways lead to positive outcomes for various cases including a reduction in the prescription of laboratory tests and in-hospital complications [36].

The limited number of resources needed to provide community health services requires optimization models and methods to aid in scheduling to best utilize the limited resources while maintaining a high quality of care for all clients. These challenges are compounded by the new paradigm of value-based purchasing [37], which has drastically changed how services are measured, reported, and rewarded in healthcare delivery. The new paradigm of healthcare delivery

asks for new designs and innovative methods to support community health service coordination and optimization. However, scheduling pathways is a very challenging problem, and literature on solution methods for this problem is scant. We are aware of a combined genetic algorithm with particle swarm optimization to schedule the clinical pathways in a hospital setting [38]. Another approach that has been considered for modeling and scheduling clinical pathways is constraint programming [39]. In this dissertation, we derived a SMIP with workload balancing model for individual CHPs scheduling.

2.3 Optimal Vaccine Allocation

In epidemiology modeling, vaccination policies depending on varying factors have been widely studied. The approaches range from deterministic to stochastic, computer simulation to statistical prediction[40, 41, 42]. Early deterministic epidemiological models on evaluating and identifying vaccination strategies to control infectious diseases were developed around the 1960s [9][43][44]. Some of these models are more focused on evaluating the predetermined vaccination strategies to see which one is more effective, and the rest emphasize more on identifying optimal vaccine allocation strategies. Ball et al. consider an optimization model in populations that mix at two levels: global mixing at a community level and local mixing at a household level [45].

Yarmand et al. and Chen et al. developed two-stage stochastic models for vaccination allocation. Yarmand et al. focuses on determining vaccine allocations in different regions [46]. The first-stage decisions prescribe vaccine distribution quantities in each region at the beginning of the epidemic, and second-stage decisions provide an opportunity to allocate additional vaccines to regions in which the outbreak has not been contained by the outcome of previous stage vaccine allocations and the magnitude of the outbreak. Chen et al. formulated a two-stage stochastic program that integrates ordering and allocation decisions [47]. The goal of their model is to minimize the cost and determine the optimal ordering and vaccine allocation plan under uncertainty in attack rate, vaccine efficacy, and demand. There are two major assumptions in their work. The first one is that the vaccine supply is unlimited. The second one is that the ordering quantity is not bounded by a budget.

Tanner et al. extended Becker and Starczak's deterministic model [48] to a stochastic setting, and developed several chance-constrained stochastic programming models to identify optimal vaccine allocation [49]. One is to minimize the total vaccine cost with a certain level of acceptance on exceeding the vaccination threshold. The second model considers minimizing the probability of the disease outbreak under a limited budget. The third model explicitly has cost and probability of the disease outbreak in the objective function. Their study assumes that no one is vaccinated yet. At the time of writing this dissertation, more than half of the population in the U.S. were fully vaccinated. Therefore, this assumption no longer holds. To capture the reality, we derived a stochastic model considers the population heterogeneity in vaccination status.

This chapter reviews three approaches of stochastic programming and related work to pathways scheduling and vaccination allocation. Based on the nature of applications and the decision maker's preference, one approach might be more suitable than the other one. In applications where the occurrence of undesired outcomes may be unavoidable and one may consider to accept such undesirable outcomes, CC and ICC approach can be applied. If infeasibility is prohibited, stochastic programming with recourse can be considered. The next chapter is about stochastic programming models.

3. PRELIMINARIES: STOCHASTIC PROGRAMMING MODELS

In this chapter, we present three models for solving problems involving uncertain parameters, including stochastic programming with recourse, CC and ICC. We also derive an extension of one-sided ICC to two-sided ICC for problems that allow violations in constraints and violations above and below target are critical.

3.1 Two-stage Stochastic Programming with Recourse

Stochastic programming is used for formulating and optimizing problems involving random parameters. The probability distribution of these parameters represents the uncertainty of the model with respect to the realization of the random parameters. The most common representation of a stochastic program's objective function uses the expectation. In this dissertation, we consider two-stage stochastic programs of the following form:

$$\begin{aligned} \text{SP2} : \text{Min } & c^\top x + \mathbb{E}[f(\tilde{\omega}, x)] \\ \text{s.t. } & Ax \geq b \\ & x \geq 0, \end{aligned} \tag{3.1}$$

where $\tilde{\omega}$ is a multivariate discrete random variable with a realization (scenario) ω with probability of occurrence p_ω and sample space Ω. $\mathbb{E}$ denotes the expectation and for an outcome ω of $\tilde{\omega}$, the recourse function $f(\omega, x)$ is given by

$$\begin{aligned} f(\omega, x) = \text{Min } & q(\omega)^\top y(\omega) \\ \text{s.t. } & W(\omega)y(\omega) \geq h(\omega) - T(\omega)x \\ & y(\omega) \geq 0. \end{aligned} \tag{3.2}$$

In formulation (3.1), x denotes the first-stage decision vector, $c \in \mathbb{R}^{n_1}$ is the first stage cost vector, $b \in \mathbb{R}^{m_1}$ is the first-stage righthand side, and $A \in \mathbb{R}^{m_1 \times n_1}$ is the first-stage constraint matrix. In the second-stage formulation (3.2), $y(\omega)$ denotes the recourse decision vector, $q(\omega) \in \mathbb{R}^{n_2}$ is the cost vector, $h(\omega) \in \mathbb{R}^{m_2}$ is the righthand side, $T(\omega) \in \mathbb{R}^{m_2 \times n_2}$ is the technology matrix, and $W(\omega) \in \mathbb{R}^{m_2 \times n_2}$ is the recourse matrix for scenario ω. If $T(\omega) = T$, for all $\omega \in \Omega$, SP2 is said to have fixed tenders. Similarly, $W(\omega) = W$, for all $\omega \in \Omega$, SP2 is said to have fixed recourse. A scenario defines the realization of the stochastic problem data $\{W(\omega), T(\omega), h(\omega)\}$. Subproblem (3.2) is generally referred to as the *scenario* problem. Formulation (3.1-3.2) can also be written in extensive form (deterministic equivalent) as follows:

$$\begin{aligned} &\text{Min } c^\top x + \sum_{\omega \in \Omega} p_\omega q(\omega)^\top y(\omega) \\ &\text{s.t. } Ax \geq b \\ &\qquad W(\omega)y(\omega) \geq h(\omega) - T(\omega)x \qquad \forall \omega \in \Omega \\ &\qquad x \geq 0, y(\omega) \geq 0. \end{aligned} \tag{3.3}$$

The decision-making process in two-stage recourse setting is illustrated in Figure 3.1. The first-stage decisions x are made without full information on the realization of the uncertain parameters. Then in the second-stage, the decisions $y(\omega)$ are made based on both the first-stage decisions and the realizations of the uncertain parameters.

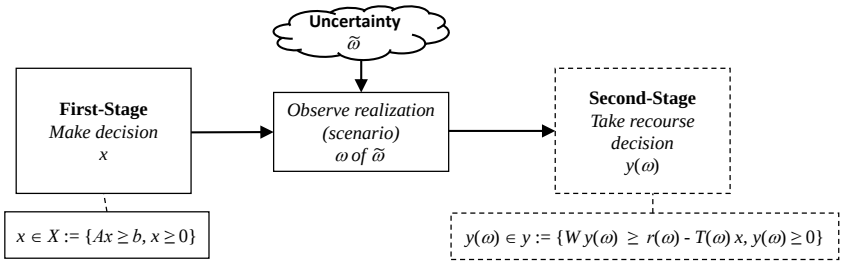

Figure 3.1: Two-stage recourse decision-making process

Let $X := \{x \in \mathbb{R}^{n_1}_+ : Ax \geq b\}$ denote the first-stage feasible set. We address instances of SP2 under the following assumptions:

(A1) The random variable $\tilde{\omega}$ follows a discrete distribution with finite support Ω and the probability of an outcome ω of $\tilde{\omega}$ is equal to p_ω.

(A2) The first-stage feasible set $X := \{x \in \mathbb{R}^{n_1}_+ : Ax \geq b\}$ is nonempty.

(A3) The second-stage feasible set $Y(\omega, x) := \{y(\omega) \in \mathbb{R}^{n_2}_+ : W(\omega)y(\omega) \geq h(\omega) - T(\omega)x\}$ is nonempty and bounded for all $x \in X$ and $\omega \in \Omega$.

3.2 Chance-constrained Stochastic Programming

Assuming that $\tilde{\omega}$ is discrete with finitely many scenarios $\omega \in \Omega$, each with corresponding probability $p(\omega)$, we can derive a (DEP) formulation for the chance constrained stochastic program. This leads the study of decomposition approaches for chance constrained stochastic programs. In this approach, the decision-maker or modeler imposes their level of acceptable risk or reliability $\alpha \in (0, 1)$. This means that the given probabilistic constraint(s) must hold $(1 - \alpha).100\%$ of the time. In practice, the typical values for α are usually between 0.95 and 1.
Consider the linear programming problem with random constraints:

$$\begin{aligned} &\text{Min } c^\top x \\ &\text{s.t. } Ax \geq b \\ &\quad \mathbb{P}\{T(\tilde{\omega})x \geq h(\tilde{\omega})\} \geq 1 - \alpha \\ &\quad x \geq 0, \end{aligned} \tag{3.4}$$

where $x \in \mathbb{R}^{n_1}$ is the decision variable vector and $T(\tilde{\omega}) \in \mathbb{R}^{m_1 \times n_1}$ is the technology matrix and $h(\omega) \in \mathbb{R}^{m_1}$ is the right hand side vector. The objective function in this case is convex in x and in many applications is in fact linear.

Let M_ω be an appropriately sized scalar for scenario ω and let e be an appropriately dimensioned vector of ones. Let us define a binary decision variable $z(\omega)$ as follows: $z(\omega) = 1$ if under

scenario w at least one of the inequalities in the probabilistic constraint is violated, and $z(\omega) = 0$ otherwise. Then a DEP formulation for problem (3.4) can be written as follows:

$$\begin{aligned} &\text{Min } c^\top x \\ &\text{s.t. } Ax \geq b \\ &\quad \mathbb{P}\{T(\tilde{\omega})x + M_\omega e z_\omega \geq h(\tilde{\omega})\} \geq \alpha \\ &\quad \sum_{\omega \in \Omega} p_\omega z_\omega \leq 1 - \alpha \\ &\quad x \geq 0, z_\omega \in \mathbb{B}, \forall \omega \in \Omega. \end{aligned} \tag{3.5}$$

The total probability of violating the probabilistic constraint is given by $\mathbb{P}\{T\tilde{\omega}x \not\geq h(\tilde{\omega})\} \leq \sum_{\omega \in \Omega} p_\omega z(\omega) \leq 1 - \alpha$. When $z(\omega) = 1$ it means that scenario ω is excluded from the CC formulation. Thus we can assume that $p_\omega \leq \alpha, \forall \omega \in \Omega$ so that the knapsack constraint (3.5) has a well-defined subset of scenarios that can be excluded from the formulation without exceeding the risk/reliability level $1 - \alpha$. The parameter $1 - \alpha$ can be thought of as a budget and that the knapsack is a budget constraint for constraint removal.

3.3 Integrated Chance Constrained Stochastic Programming

ICC is a modeling tool for here-and-now stochastic programming problems.

$$\begin{aligned} f(\omega, x) = \text{Min } & c^\top x \\ \text{s.t. } & T(\omega)x = h(\omega) \\ & x \in X, \end{aligned} \tag{3.6}$$

where $X := \{x \in \mathbf{R}^n_+ : Ax = b\}$.

There are m random constraints $T_i(\omega)x = h_i(\omega), i \in I := \{1, ..., m\}$, where $T_i(\omega)$ is the $i-$th row of matrix $T(\omega)$, and $h_i(\omega)$ is the $i-$th component of vector $h(\omega)$. Let's define $\eta_i(x, \omega) :=$

$T_i(\omega)x - h_i(\omega), \forall i \in I$, and $\eta_i(x,\omega)^- := \max\{0, -\eta_i(x,\omega)\}$. In this dissertation, we define $\eta_i(x,\omega)^-$ as shortage. Constraints in formulation (3.6) avoid any positive shortage, however it might not be impossible to exclude shortage completely due to the randomness in $h(\omega)$ and $T(\omega)$. In the situation, where the amount of shortage is critical, we can use *mean shortage* $\mathbb{E}_\omega[\eta_i(x,\omega)^-]$ and bounded by a fixed risk aversion parameter β_i:

$$X_1(\ \beta_i) := \{x \in X : \mathbb{E}_\omega[\eta_i(x,\omega)^-] \leq \beta_i\}, \beta_i \in [0, \infty]$$

For example, in production planning this measure of positive shortage is the deficiency to satisfy the demand $h(\omega)$ in a time period, and the expected shortage must be limited by a certain amount β_i. Let z^i_ω represent the positive shortage for ith constraint. Integrated chance-constrained problems with finite discrete distribution can be represented in the LP form as follows:

$$\begin{aligned}
&\text{Min } c^\top x \\
&\text{s.t. } T_i(\omega)x_+ z_i(\omega) \geq h_i(\omega), \forall i = 1, ..., I \\
&\quad \sum_{\omega=1}^{\Omega} p(\omega) z_i(\omega) \leq \beta_i, \forall i = 1, ..., I \\
&\quad z_i(\omega) \geq 0, \forall \omega \in \Omega, i \in 1, ..., I \\
&\quad x \in X, X := \{x \in \mathbf{R}^n_+ : Ax = b\}.
\end{aligned} \tag{3.7}$$

This DEP formulation has additional $|\Omega| + 1$ constraints and $|\Omega|$ variables. Solving DEP for instances with large number of scenarios is computationally demanding. In the next subsection, a reduced form algorithm is introduced to solve ICC.

Reduced Form Algorithm for Integrated Chance Constrained Program

As mentioned in the previous section, the ICC DEP can be computationally demanding when more scenarios are involved in an instance. Haneveld and Vlerk introduced a reduced form algorithm to efficiently solve ICC problems [11]. The detailed steps are shown as follows:

Step 0. Initialization: $\bar{T} = \sum_{s=1}^{S} p(\omega^s)T(\omega^s)$, $\bar{h} = \sum_{s=1}^{S} p(\omega^s)h(\omega^s)$, $\beta > 0$ and $\mathcal{C}^0 := \{x \in \mathbb{R}^n : \bar{T}x \geq \bar{h} - \beta\}$. Let iteration index $t = 0$.

Step 1. Define and Solve Current Problem:

$$\begin{aligned} f(x) := \text{Min} \quad & c^\top x \\ \text{s.t.} \quad & x \in X \\ & x \in \mathcal{C}^t, \end{aligned}$$

Step 2. Solve the LP problem CP: If CP is infeasible, stop. Problem is infeasible. If feasible, get incumbent solution x^t.

Step 3. Compute the shortage: Compute $\mathbb{E}_\omega[\eta(x^t, \omega)^-] = \sum_{s=1}^{S} p(\omega^s)\eta(x^t, \omega^s)^-$, and set $K^t := \{s \in S : \eta(x^t, \omega^s)^- > 0\}$.

Step 4. Add feasibility cut and solve:

If $\mathbb{E}_\omega[\eta(x^t, \omega)^-] \leq \beta$, stop: x^t is an optimal solution.

Otherwise, construct feasibility cut $d_{t+1}x \leq e_{t+1}$, where $d_{t+1} = -\sum_{k \in K^t} p^k T^k$, $e_{t+1} = \beta - \sum_{k \in K^t} p^k h^k$. Set $\mathcal{C}^{t+1} = \mathcal{C}^t \cap \{x \in \mathbb{R}^n : d_{t+1}x \leq e_{t+1}\}$. Set $t \leftarrow t + 1$, and return to Step 1.

Two-sided Integrated Chance-constrained Programming

Stochastic programming with recourse, CC and ICC approaches are presented in Section 3.1, 3.2 and 3.2. Those approaches are the foundations to develop two-sided ICC. In this subsection, two-sided ICC formulation and its DEP are derived. For instances with a large number of scenarios, a decomposition algorithm for two-sided ICC is provided in Subsection 3.3.

Let us define a general formulation for two-side ICC problems.

$$\begin{aligned} f(\omega, x) = \text{Min } & c^\top x \\ \text{s.t. } & T(\omega)x = h(\omega) \\ & x \in X, \end{aligned} \tag{3.8}$$

where $X := \{x \in \mathbf{R}^n_+ : Ax = b\}$.

There are m random constraints $T_i(\omega)x = h_i(\omega), i \in I := \{1, ..., m\}$, where $T_i(\omega)$ is the $i-$th row of matrix $T(\omega)$, and $h_i(\omega)$ is the $i-$th component of vector $h(\omega)$. Let's define $\eta_i(x, \omega) := T_i(\omega)x - h_i(\omega), \forall i \in I$, $\eta_i(x, \omega)^- := \max\{0, -\eta_i(x, \omega)\}$ and $\eta_i(x, \omega)^+ := \max\{0, \eta_i(x, \omega)\}$. In this dissertation, we refer $\eta_i(x, \omega)^-$ as shortage and $\eta_i(x, \omega)^+$ as excess.

Constraints in formulation (3.8) avoids any positive shortage or excess. In certain applications, shortages and excesses are unavoidable due to the randomness in parameters. In the situation, where the amount of excesses and shortages is critical, we can use *mean shortage* $\mathbb{E}_\omega[\eta_i(x, \omega)^-]$ and *mean excess* $\mathbb{E}_\omega[\eta_i(x, \omega)^+]$ and bound them by fixed risk aversion parameter β_i and α_i respectively.

$$X_1(\beta_i) := \{x \in X : \mathbb{E}_\omega[\eta_i(x, \omega)^-] \leq \beta_i,\ \mathbb{E}_\omega[\eta_i(x, \omega)^+] \leq \alpha_i\},\ \beta_i \in [0, \infty],\ \alpha_i \in [0, \infty]$$

Let z^i_ω represent the positive shortage and e^i_ω represent the positive excess for $i-$th constraint. ICC with finite discrete distribution can be represented in the LP form as follows:

$$\begin{aligned}
&\text{Min } c^\top x \\
&\text{s.t. } T_i(\omega)x + z_i(\omega) - e_i(\omega) = h_i(\omega), \forall i = 1, ..., I \\
&\quad \sum_{\omega=1}^{\Omega} p(\omega) z_i(\omega) \leq \beta_i, \forall i = 1, ..., I \\
&\quad \sum_{\omega=1}^{\Omega} p(\omega) e_i(\omega) \leq \alpha_i, \forall i = 1, ..., I \\
&\quad z_i(\omega), e_i(\omega) \geq 0, \forall \omega \in \Omega, i \in 1, ..., I \\
&\quad x \in X, X := \{x \in \mathbf{R}^n_+ : Ax = b\}.
\end{aligned} \tag{3.9}$$

Assume that ω is a discrete random vector, with $\Pr\{\omega = \omega^s\} = p^s, s \in S$, and let $(l^s, h^s) = (l(\omega^s), h(\omega^s))$, for $s \in S$. Then, for $\beta \geq 0$,

$$C_1(\beta) = \cap_{K \subseteq S} \{x \in \mathbb{R}^n : \sum_{k \in K} p^k (h^k - T^k x) \leq \beta\} \tag{3.10}$$

For $\alpha \geq 0$,

$$C_1(\alpha) = \cap_{K \subseteq S} \{x \in \mathbb{R}^n : \sum_{k \in K} p^k (T^k x - h^k) \leq \alpha\} \tag{3.11}$$

If S is a finite set, then $C_1(\beta)$ is a polyhedral set defined by $2^{|S|} - 1$ linear constraints and $C_1(\alpha)$ is a polyhedral set defined by $2^{|S|} - 1$ linear constraints.

Two-sided ICC Algorithm

As mentioned in the previous section, the ICC DEP can be computationally demanding when more scenarios are involved in an instance. The following two-sided reduced form algorithm is derived based Haneveld and Vlerk ICC algorithm presented in Section 3.3. The two-sided ICC algorithm iteratively adds cuts to reach the optimal solution. The detailed steps are shown as follows:

Step 0. Initialization: $\bar{T} = \sum_{s=1}^{S} p(\omega^s) T(\omega^s)$, $\bar{h} = \sum_{s=1}^{S} p(\omega^s) h(\omega^s)$, $\beta > 0$, $\mathcal{C}^0 := \{x \in \mathbb{R}^n : \bar{T}x \geq \bar{h} - \beta\}$ and $\mathcal{D}^0 := \{x \in \mathbb{R}^n : \bar{T}x \leq \bar{h} + \alpha\}$. Let iteration index $t = 0$.

Step 1. Define and Solve Current Problem:

$$\begin{aligned} f(x) := \text{Min} \quad & c^\top x \\ \text{s.t.} \quad & x \in X \\ & x \in \mathcal{C}^t \\ & x \in \mathcal{D}^t \end{aligned}$$

Step 2. Solve the LP problem CP: If CP is infeasible, stop. Problem is infeasible. If feasible, get incumbent solution x^t.

Step 3. Compute the shortage and excess:

Compute $\mathbb{E}[\eta(x^t,\tilde{\omega})^-] = \sum_{s=1}^{S} p(\omega^s)\eta(x^t,\omega^s)^-$,$\mathbb{E}[\eta(x^t,\tilde{\omega})^+] = \sum_{s=1}^{S} p(\omega^s)\eta(x^t,\omega^s)^+$, and at the same time constructing the index sets

$$K^t := \{s \in S : \eta(x^t,\omega^s)^- > 0\},$$

$$L^t := \{s \in S : \eta(x^t,\omega^s)^+ > 0\}.$$

Step 4. Add feasibility cut and solve: If $\mathbb{E}[\eta(x^t,\tilde{\omega})^-] \leq \beta$ and $\mathbb{E}[\eta(x^t,\tilde{\omega})^+] \leq \alpha$, stop: x^t is an optimal solution.

Step 4.1 If $\mathbb{E}[\eta(x^t,\tilde{\omega})^-] \geq \beta$, construct feasibility cut $d_{t+1}x \leq e_{t+1}$, where

$$d_{t+1} = -\sum_{k\in K^t} p^k T^k, \qquad e_{t+1} = \beta - \sum_{k\in K^t} p^k h^k,$$

and set

$$\mathcal{C}^{t+1} = \mathcal{C}^t \cap \{x \in \mathbb{R}^n : d_{t+1}x \leq e_{t+1}\}.$$

Step 4.2 If $\mathbb{E}[\eta(x^t,\tilde{\omega})^+] \geq \alpha$, construct feasibility cut $l_{t+1}x \leq r_{t+1}$, where

$$l_{t+1} = \sum_{k\in L^t} p^k T^k, \qquad r_{t+1} = \alpha + \sum_{k\in L^t} p^k h^k,$$

and set

$$\mathcal{D}^{t+1} = \mathcal{D}^t \cap \{x \in \mathbb{R}^n : l_{t+1}x \leq r_{t+1}\}.$$

Step 4.3 Set $t \leftarrow t+1$, and return to Step 1.

Two-sided ICC Algorithm convergence proof

Since ω is discretely distributed, if we can find some $x \in X$ where $C_1(\beta, x)$ is a nonempty set, then we have

$$\mathbb{E}[\eta(y(\tilde{\omega})^-)] = \sum_{s\in S} p^s \max\{0, -\eta(x,\omega^s)\} \tag{3.12a}$$

$$= \sum_{s\in S} \max\{0, -p^s\eta(x,\omega^s))\} \tag{3.12b}$$

$$= \sum_{s\in S} (-p^s\eta(x,\omega^s))^+ \tag{3.12c}$$

$$= \max_{K\subseteq S} \sum_{k\in K} -p^k\eta(x,\omega^s). \tag{3.12d}$$

Therefore, we have

$$C_1(\beta) = \cap_{K\subseteq S}\{x\in\mathbb{R}^n : -\sum_{k\in K} p^k\eta(y^k) \le \beta\} \tag{3.12e}$$

$$= \cap_{K\subseteq S}\{x\in\mathbb{R}^n : \sum_{k\in K} p^k(h^k - T^k x) \le \beta\}. \tag{3.12f}$$

If S is finite, then there are $2^{|S|}-1$ nonempty subsets of S, so that (3.11) describes the convex set $C_1(\beta)$ using finitely many linear constraints. That is $C_1(\beta)$ is a polyhedral set in this case.

Now, we show that the $C_1(\alpha)$ is a polyhedral set defined by $2^{|S|}-1$ linear constraint.

$$\mathbb{E}[\eta(y(\tilde{\omega})^+)] = \sum_{s\in S} p^s \max\{0, \eta(x,\omega^s)\} \tag{3.13a}$$

$$= \sum_{s\in S} \max\{0, p^s\eta(x,\omega^s))\} \tag{3.13b}$$

$$= \sum_{s\in S} (p^s\eta(x,\omega^s))^+ \tag{3.13c}$$

$$= \max_{K\subseteq S} \sum_{k\in K} p^k\eta(x,\omega^s). \tag{3.13d}$$

Therefore, we have

$$C_1(\alpha) = \cap_{K\subseteq S}\{x\in\mathbb{R}^n : \sum_{k\in K} p^k\eta(y^k) \le \alpha\} \tag{3.13e}$$

$$= \cap_{K\subseteq S}\{x\in\mathbb{R}^n : \sum_{k\in K} p^k(T^kx - h^k) \le \alpha\}. \tag{3.13f}$$

Remark 1 For $K = S$ in (3.12), we obtain $\bar{T} \ge \bar{h} - \beta$, where $\bar{T} := \mathbb{E}[T(\tilde{\omega})]$ and $\bar{h} := \mathbb{E}[h(\tilde{\omega})]$. Because $T(\omega)$ and $h(\omega)$ depend linearly on ω, this is equivalent to $\eta(x, \mathbb{E}[\tilde{\omega}])^- \le \beta$. This is an obvious necessary condition for $x \in C_1(\beta)$, since $\eta(x,\omega)^- \ge -\eta(x,\omega)$ for all ω so that $\mathbb{E}[\eta(x,\tilde{\omega})] \ge -\eta(x, \mathbb{E}[\tilde{\omega}])$.

4. COMMUNITY HEALTH PATHWAYS SCHEDULING

Scheduling and coordinating constrained resources in community healthcare settings at a centralized Pathways Community HUB is challenging due to limited resources and the inherent dynamics of the processes and the organizational structures. In this chapter, we introduce a stochastic programming approach for connected community health for optimally scheduling community health pathways (CHPs) under uncertainty in resource availability. A CHP is a standardized tool that details multiple steps of a healthcare-related service and the required resources for each step. The new methodology was implemented and applied to data for a real Pathways Community HUB for a U.S. county involving a number of CHPs, community health workers, physicians, and other resources. The computational study shows that client access time depends on the HUB resources uncertain future availability and client demand, with high client demand resulting in longer access time. The study reveals several managerial insights, including the observation that workload balancing is beneficial in terms of providing schedules that are equitable across the same type of community health workers with access times that are comparable to the when no workload balancing is considered.

4.1 Introduction

Community healthcare agencies in the U.S. such as those at the county level are tasked with providing medical, behavioral, and social services to community members in need. However, providing such services requires careful coordination of limited resources. Agency resources include case managers, community health workers, and office facilities, while external resources include physicians, nurses, social workers, behavioral health specialists, insurance companies, and community-based organizations. Care coordination is the organization of care activities among individual clients and providers to facilitate the appropriate delivery of healthcare services [32]. Performing care coordination involving disparate resources presents significant challenges in terms of scheduling, adhering to the care activities protocols, and tracking progress of these activities for

each client in the system. The focus of this chapter is on community care coordination using the *Pathways Community HUB* model of care coordination [4]. This model considers the community level to improve quality of care for individual clients by coordinating community-based health and social services.

This work introduces a stochastic programming (SP) approach for scheduling and coordinating community health pathways (CHPs) under uncertainty in the availability of the limited HUB resources and client demand, while providing equity among community health workers via workload balancing. There are different types of pathways and in this work we focus on CHPs for connected community health services, which are different from *clinical* or *care* pathways [50]. A CHP is simply a structured and time-framed multidisciplinary care guideline that details essential steps of a community healthcare process. It provides a sequence of appointments and resources needed for each appointment together with its duration over a specified time horizon. CHPs are unique in that they track the individual client being served and each step of the CHP addresses a well defined action towards resolving the issue addressed by the pathway. Such issues include lack of health insurance, medical home, homelessness, pregnancy, immunizations, and so on. Each step can deal with a health, social or cultural issue. A CHP is not considered complete until the issue is successfully resolved or until a specific point is reached to close in a documented manner that the CHP that has not been completed. In addition, CHPs are associated with payment for specific benchmarks along the pathway with the highest payment given for a successful outcome at completion of the pathway.

The Pathways Community HUB model of care coordination is a construct that was introduced to enable coordination of care activities of different organizations and their services. Pathway models focus on the progress and outcomes of individual clients as they traverse the care organizations [35]. In turn, pathways coordination can enable a comprehensive approach to community health service focused on reducing the healthcare inequalities to improve health outcomes for the community. Community-based services have been shown to play a vital role in addressing some of the nation's most difficult health problems, including health disparities and the rising chronic

health conditions such as obesity and diabetes [33]. Effective care coordination at the community level is a hard task. Many individuals who need community health services have complex health needs and chronic health conditions [51]. Addressing these complex needs requires a combination of multiple services (medical services, behavioral health services, and social services) and support from a wide variety of community-based resources in order to reduce the health and social barriers to improve healthcare outcomes [34]. This complexity poses major challenges in terms of effectively connecting the different parties (clients, agencies, service providers) and coordinating them to work in concert to achieve positive outcomes.

The limited number of resources needed to provide community health services calls for optimization models and methods to aid in scheduling to best utilize the limited resources while providing quick access time for all clients. This scheduling challenge is compounded by the new paradigm of value-based purchasing [37], which has drastically changed how services are measured, reported, and rewarded in healthcare delivery. The new paradigm of healthcare delivery asks for new designs and innovative methods to support community health service coordination and optimization. This work makes a step toward achieving that goal. However, scheduling CHPs is a very challenging problem and literature on solution methods for this problem is scant. The few available works are in the hospital setting: constraint programming model [39] and combined genetic algorithm with particle swarm optimization for scheduling clinical pathways in a hospital setting [38]. The work of [38] shows that clinical pathways can significantly improve patient waiting time in a hospital setting. Furthermore, studies have shown that clinical pathways lead to positive outcomes for various cases, including a reduction in the prescription of laboratory tests [52] and in-hospital complications [36].

Recent work on scheduling in the general healthcare setting include a physician mixed-integer programming (MIP) scheduling model to assign physicians to overnight duties based on their preferences and incorporate fairness based on our satisfaction indicator [53], a mixed integer robust optimization approach for scheduling patient appointment in an infusion center [54], and a radiotherapy treatment scheduling model considering time window preferences [55]. The work by [56]

considers schedule configuration of a hybrid appointment system for a two-stage outpatient clinic with multiple servers. Patient scheduling in outpatient clinics under demand uncertainty has also been considered to minimize patient waiting times [57].

The main contributions of this chapter include the following: a) an SP model for optimally scheduling individual CHPs under unknown future resource availability while allowing for workload balancing of resources of the same type to enable equity among personnel; b) a Monte Carlo simulation model that uses the SP model to assess CHPs scheduling and workload balancing in a structured setting. This model-based approach allows for progress tracking and notification for individual CHPs as well as computing and monitoring of system performance measures over time; and c) a computational study based on a real setting to demonstrate the new approach and gain managerial insights into CHPs scheduling under uncertainty in resource availability and different client demand scenarios.

The rest of this chapter is organized as follows: In the next section we describe the materials and methods used in this work, including data collection and analysis, model development and implementation, experiment design, and the SP pathway scheduling model. Next, we report on simulation results followed by a discussion and concluding remarks and future work.

4.2 Materials and Methods

Motivated by a real Pathways Community HUB, we developed a computer simulation model to mimic client appointment requests arrivals for CHPs, scheduling CHPs, and the arrival of clients at the HUB for their appointment. The goal of the simulation model was to help us gain managerial insights into the computational performance of the stochastic programming (SP) approach under different demand cases and resource availability scenarios. Next, we describe our data collection and analysis, including the real setting and design of experiments. We devote most of the space to deriving the SP pathway scheduling model.

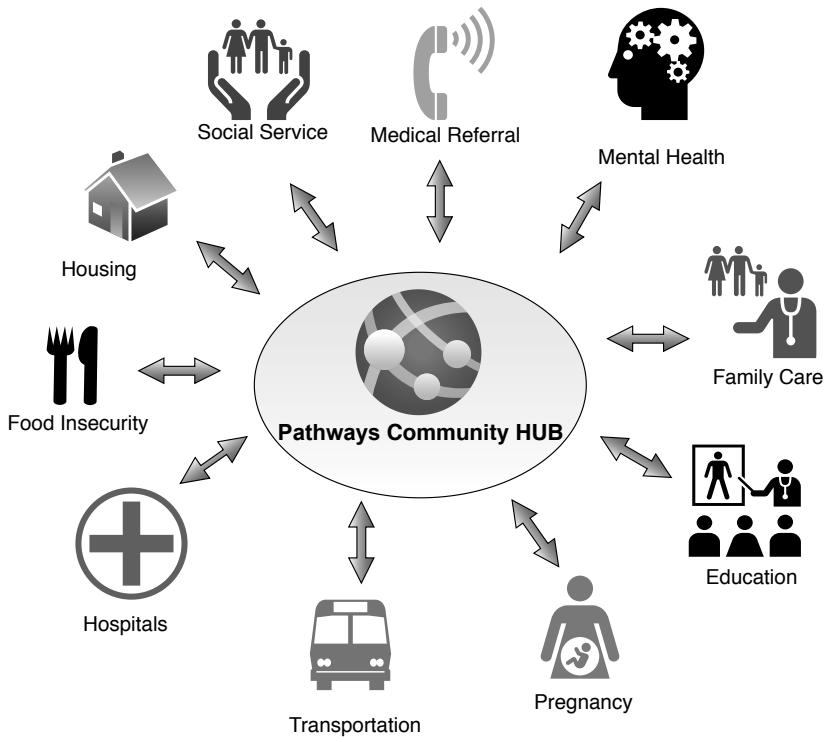

Figure 4.1: Pathways Community HUB Model

4.2.1 Data Collection and Analysis

The Pathways Community HUB setting we consider is a county on the east coast of the U.S. This HUB provides a delivery system for care coordination services in a community setting with a goal of improving health outcomes for the high-risk and providing preventive care in the county. For some programs community-based coordination simply refers to transition from a medical facility (e.g., a hospital) to the community (e.g., residence or nursing home). However, in this case community involvement is not only limited to the patient's residence or nursing home, but care coordination involves multiple providers and multiple services within a larger community setting as depicted in Figure 4.1. In this HUB, CHPs serve as a documentation and reporting tool that capture a set of guiding principles for finding those at risk, ensuring that they are treated with evidence-based medical and social interventions, and measuring the health outcomes and costs of these efforts. In essence, this supplements clinical services with the social services needed to

overcome social barriers to healthcare for those most at risk [4].

CHPs include both health and social issues that need to be addressed with a goal of increasing the likelihood of a positive outcome for the client. The purpose of the HUB is to provide a central point for registry and outcome tracking. It connects community care coordination agencies, providers, and payers, and uses pathways along with defined metrics to track progress at the individual level, care coordinator, agency, and regional level. In terms of service payments, pathways are associated with payment for specific benchmarks along the CHP through to successful outcomes at completion. Therefore, CHPs provide the ability to link payment to outcomes and thus enabling linking payments to performance.

The HUB deals with about 40,000 residents with over 90% of the population belonging to a racial or ethnic minority group. Population diversity and lack of reliable data on residents' healthcare needs make it more challenging for the county to provide timely access to appropriate healthcare services. The community care coordination team established a management model using CHPs at the community health county level to improve the healthcare outcomes. The HUB operates nine hours a day from 8:00 am to 5:00 pm, Monday through Friday, with one hour lunch break from 12:00 pm to 1:00 pm. It has several behavioral, social and medical CHPs, 20 of which are listed in Table 4.1. We give an example of the Insurance CHP in Figure 4.2 in the Appendix.

When residents (we refer to them as *clients*) need health related services, the HUB clinical health workers (CHWs) use CHPs as guidelines to establish communications among stakeholders, such as the hospital, educational institutions, insurers and health care providers. CHWs identify which CHPs are appropriate for each client and allocate resources to all steps of the assigned CHPs within specified time frame. However, it is very challenging to find the earliest first appointment due to the uncertain future availability of the resources for all the steps of a CHP as well as the limited number of CHWs. When the CHP assigned to a client cannot be scheduled within 10 days, the CHW will issue a referral to the client to seek another community health center. There are nine types of resources at this HUB listed in Table 4.2, each with the specific number we used in our computational study.

	CHP Name	Abbreviation	Days	Steps
1	Acute Coronary Syndrome	ACS	22	6
2	Asthma	ASM	25	6
3	Behavioral Health Intervention	BHI	25	6
4	Care Team	CAT	25	4
5	Companion or Care Attendant	CCA	15	5
6	Closed Head Injury	CHI	20	4
7	Caesarean Birth	CSB	9	6
8	Domestic Violence	DMV	25	6
9	Dietitian and Nutrition Consultant	DNC	22	6
10	Dying Person Care	DPC	17	5
11	Food Insecurity	FDI	25	7
12	Housing	HUS	23	5
13	Insurance	INS	25	6
14	Medical Home	MDH	10	6
15	Medical Referral	MDR	14	3
16	Prime Time Sister Circle	PTS	25	8
17	Smoking Cessation	SMC	25	6
18	Social Service Referral	SSR	25	6
19	Thrombolysis	TBS	15	6
20	Transportation-HEZ	TRH	3	3

Table 4.1: Community Health Pathways (CHPs) available in the HUB

	Resource Name	Abbreviation	Number
1	Patient Navigator	PNT	3
2	Educator	EDU	4
3	Liaison	LAS	3
4	Outreach Worker	OTW	4
5	Patient Counselor	PEC	5
6	Health Interpreter	HIP	4
7	Training Location	TRL	5
8	Community Health Advisor	CHA	4
9	Transporter	TRS	3

Table 4.2: Resource types available in the HUB

The Insurance CHP in Figure 4.2 takes 25 days to complete and involves six steps after initiation: step 1 (Investigate) on day 1 requires one resource, CHA, for one 15-minute timeslot; step 2 (Application) on day 2 requires one resource, OTW, for two 15-minute timeslots; step 3 (Appointment, Education) on day 7 requires three resources, OTW for one 15-minute timeslot and EDU and

TRL for two 15-minute timeslots concurrently and ; step 4 (Processing) on day 14 requires one resource, HIP, for one 15-minute timeslot and ; step 5 (Processing Verification) on day 21 requires one resource, HIP; and step 6 (Completion) on day 25 requires one resource, PEC.

4.2.2 Model Development and Implementation

Managing clients and resources in the HUB in extremely challenging, especially as relates to scheduling clients for different pathways using limited resources whose future availability is uncertainty. We developed an SP pathway scheduling model together with a simulation model of the HUB to evaluate the performance of the SP approach. The computer simulation and SP models were coded in the CPLEX 12.9 Callable Library [58] using C++ and all experiments were performed on a Dell Precision with a Quad Core 2395 MHz processor and 12.0GB RAM. The computer simulation model has a client generator and a CHP scheduler as depicted in Figure 4.3. The Client Generator creates client arrivals on each day of the planning horizon. Clients arrive one at a time and request services, and CHPs are assigned based on each client's request and needs as determined by the CHW. Then the Scheduler searches for the earliest possible appointment for the assigned CHP that gives minimum workload imbalance, if workload balancing is selected. The future availability of the resources that are assigned to the CHP steps is updated by the Resource Allocator according to the assigned resources. If the assigned CHP cannot be scheduled within 10 days, it is recorded as not scheduled and the client leaves the simulation.

After scheduling a CHP for a client, Client Generator generates the next client to request services. The simulation ends, when the last client is scheduled on the last appointment day. The HUB hours of operation are divided into 15-minute timeslots, and the CHP steps are assigned to timeslots. Thus, there are 32 working timeslots each day with four break timeslots from 12:00 pm to 1:00 pm.

4.2.3 Experimental Design

We conducted several experiments to assess the schedules determined by the SP model over a specified time horizon to gain managerial insights. Specifically, we wanted to to study the fol-

Insurance Pathway: 25-days

Client Name
Date of Birth
Address/Phone
Primary Diagnosis
Pathway Start Date

Step	Day	Activity	Sub-Activities	RES1	RES2	RES3	Order
0		Initiation	Client is uninsured and needs health insurance				
1	1	Investigate	1. Investigate insurance resources 2. Discuss the insurance coverage 3. Discuss the options with client 4. Make the selection	CHA 15	0	0	{0}
2	2	Application	1. Assist client with the application 2. Submit application and verify the date	OTW 30	0	0	{0}
3	7	Appointment Education	1.1 Set appointment with provider 1.2 Date and time of appointment: 1.3 Date client informed of scheduled appointment with _____ Insurance 1.4 Location of appointment 1.5 Contact person: _____ 2.1 Client educated about the importance of having Insurance. 2.2 Client educated. 2.3 Provide Client Tips on how to check on the status of your application 2.4 Date education provided _____	OTW 15	EDU 30	TRL 30	{0,1,1}
4	14	Processing	Status check	HIP 15	0	0	{0}
5	21	Processing Verification	1.1 Status check 2.1 Did client keep the scheduled appointment to review application and supporting documents. Yes / No 2.2 Verification: Informed by client /by Agency Contact /On-line confirmation	HIP 15	0	0	{0}
6	25	Completion	Insurance Denied ___ Client did not complete process ___ Date of completion ___ OR Follow up needed ___	PEC 15	0	0	{0}

Figure 4.2: The Insurance CHP

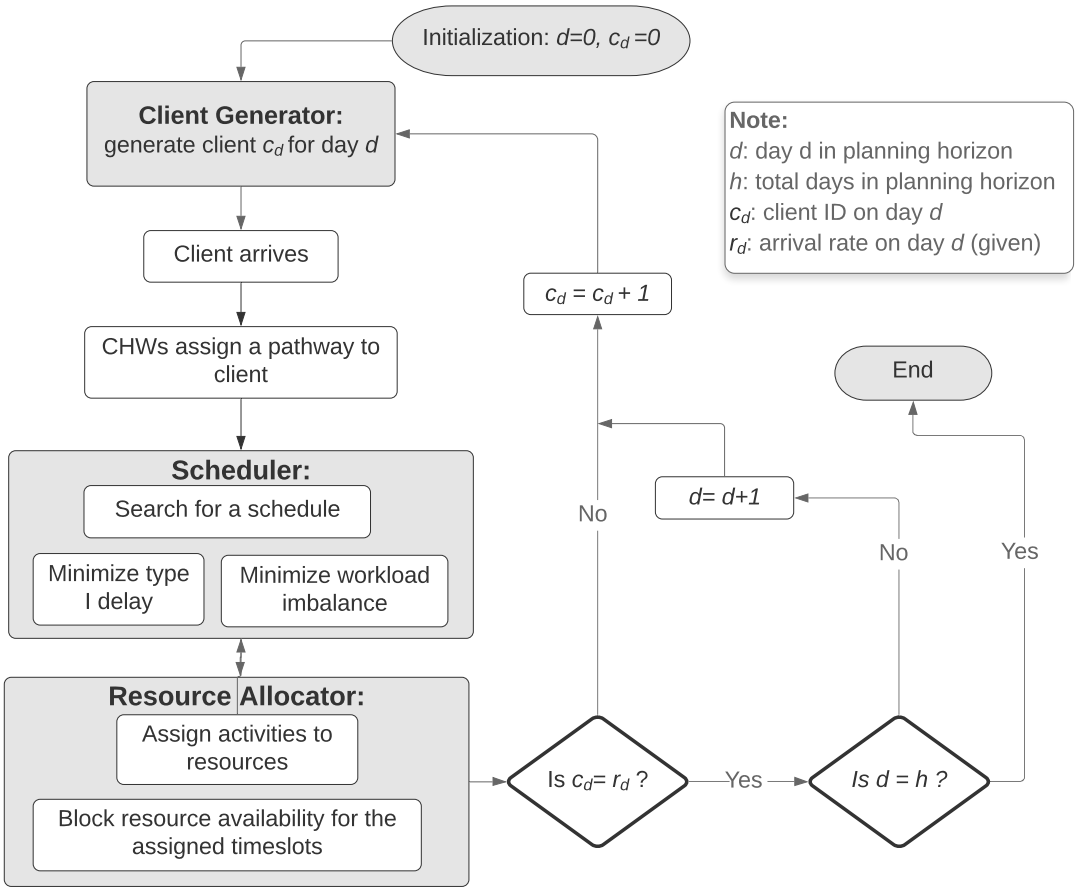

Figure 4.3: CHP scheduling simulation flowchart

lowing *four main aspects* of CHPs scheduling under uncertainty: a) variation of client acess time; b) resource utilization; c) workload balancing (WB) versus no workload balancing (NWB); and d) impact of client demand on scheduling.

We considered the following performance measures: access time, number of clients not scheduled, number of clients who have to wait at least one day, workload in terms of the number of timeslots assigned to a resource, workload coefficient of variation (CV), and minimum, mean and maximum workload.

Client request daily arrival rate is a critical factor in scheduling CHPs. It translates into client demand volume, which significantly affects scheduling decisions in terms of client access time. Therefore, we experimented with three cases: *low demand* (Case I), *medium demand* (Case II) and

high demand (Case III). Demand volume is determined by client daily arrival rate at the HUB. Since daily arrival rate is stochastic, we assumed *uniform* ($\mathcal{U}$) distributions given in Table 4.3. The parameters were set based on estimates for the HUB used in this study. Clients were set to be scheduled over the first 75 days (*appointment days*) of a planning horizon of 100 business days, i.e., four months. All the three cases had the same resource types (given in Table 4.2) each with its uncertainty availability following the *Bernoulli* ($\mathcal{B}$) distribution as given in Table 4.3. We set the number of scenarios as shown in the table. Both the number of scenarios and resource availability $\mathcal{B}$ distribution p values was carefully set based on the HUB characteristics. Recall that for each scenario, the availability of each resource for each of the 32 timeslots per day for 100 days has to be specified.

Table 4.3: Experiment cases and settings

				Case I	Case II	Case III			
Demand				*Low*	*Medium*	*High*			
Client daily arrival rate				$\mathcal{U}(5,15)$	$\mathcal{U}(15,25)$	$\mathcal{U}(25,35)$			
Number of scenarios				10	10	5			
Res Type	PNT	EDU	LAS	OTW	PEC	HIP	TRL	CHA	TRS
p value	0.9	0.9	0.9	0.9	0.9	0.9	1.0	0.9	1.0

We performed three replications for each demand case to guard against spurious cases and recorded the average (mean) for all the performance measures, and in some cases we also recorded the minimum and maximum values. We first investigated the impact of using deterministic (assumed to be known) resource availability versus stochastic resource availability on the performance measures. We specifically compared the results of the WB and NWB settings to evaluate equity issues among CHW resources of the same type.

4.3 CHPs Scheduling Model

A CHP involves several steps with each step requiring one or more resources and the required resource(s) for each step have to be scheduled for a specific day and time. This involves scheduling

multiple care activities that have to be processed at some point between an earliest start time and a latest completion time, all while satisfying the required resources' availability constraints. For example, if a CHP step needs three resources to perform three different activities in order, the earliest starting time for the second resource has to be no earlier than the end of first activity. Furthermore, the latest completion time for the second activity has to leave enough time for the third resource to perform the last activity. The CHPs scheduling problem belongs to the set of parallel machine scheduling problems with limited resources and is challenging to solve.

We devise a two-stage stochastic programming (SP) formulation of the problem under unknown future resources' availability for determining optimal schedules (appointments) that provide minimum waiting (access) time and equitable workload among the resources. In the first-stage, we determine here-and-now the client's schedule for all the steps in the CHP, i.e., we assign a day, timeslots and required resources for each step of the CHP before availability of the resources is unveiled. Then in the second-stage we account for possible future resource availability for each day and step of the CHP to inform the first-stage in finding an optimal schedule. In this SP approach the unknown future availability of the resources is characterized by probability distributions. Specifically, we consider a probability distribution for the availability of each resource for each day and each timeslot, respectively, in the future.

The SP approach enables to schedule resources in the first-stage such that those resources are most likely to be available in the future for each step of the CHP to minimize potential appointment cancellations. We should point out that in reality one can think of finding another resource to substitute the unavailable resource at the same of the appointment. However, community healthcare service is often burdened with scheduling large volumes of the clients under limited resources. Thus a planning tool to aid determining appointments that are unlikely to be canceled is essential. To formulate the SP model for scheduling a client appointment for a given CHP, we use the following mathematical notation:

First-Stage Sets

$\mathcal{P}$:	Set of CHPs, indexed p.
$\mathcal{R}(i)$:	Set of resources of type i, indexed r.
$\mathcal{I}(p)$:	Set of resource types needed for CHP p, indexed i.
$\mathcal{I}(p,s)$:	Set of resource types needed for step s of CHP p, indexed i.
$\mathcal{S}(p)$:	Set of steps for CHP p, indexed s.
$\mathcal{T}$:	Set of timeslots in a day, indexed t.
$\mathcal{D}$:	Set of days in the planning horizon, indexed d.
$\mathcal{D}(p)$:	Subset of days in the planning horizon on which CHP p can start, indexed d.
$\bar{\mathcal{D}}(p,d)$:	Given a CHP p starting on day $d \in \mathcal{D}(p)$, $\bar{\mathcal{D}}(p,d)$ is the set of CHP calendar days for all steps of CHP p, indexed h.
$\mathcal{O}(p,s)$:	$\mathcal{O}(p,s)$ is a set of numbers indicating the resource sequence order for step s of CHP p.

First-Stage Parameters

c_d:	Cost of starting appointment on day d.
$a_{p,s,i,r,t,h}$:	$a_{p,s,i,r,t,h} = 1$, if resource r of type i is available for step s of CHP p at start timeslot t on day h of CHP calendar, $a_{p,s,i,r,t,h} = 0$, otherwise.
$n_{p,s,i}$:	$n_{p,s,i}$ is the number of consecutive timeslots using resource type i for step s of CHP p.
$b_{i,r,h}$:	$b_{i,r,h}$ is the total number of timeslots that resource r of type $i$is already assigned on day h when schedule .
ES_r:	ES_r is earliest starting time for type i resource $r \in \mathcal{R}(i)$.
LS_r:	LS_r is latest starting time for type i resource $r \in \mathcal{R}(i)$.
EA_r:	EA_r is earliest assigned time for type i resource $r \in \mathcal{R}(i)$.
LA_r:	LA_r is latest assigned time for type i resource $r \in \mathcal{R}(i)$.

First-Stage Decision Variables

z_d:	$z_d = 1$, if client starts the first appointment on day d ofthe planning horizon, $z_d = 0$, otherwise.
z:	Vector of z_d's, $z = (z_1, \cdots, z_{\|\mathcal{D}(p)\|})$.
$x_{p,s,i,r,h}$:	$x_{p,s,i,r,h} = 1$, if resource r of resource type i is assigned to step s of CHP p on day h, $h \in \bar{\mathcal{D}}(p,d)$, $x_{p,s,i,r,h} = 0$, otherwise.
x:	Vector of $x_{p,s,i,r,h}$'s.
$y_{p,s,i,r,t,h}$:	$y_{p,s,i,r,t,h} = 1$, if resource r of type i required for step s of CHP p is assigned to timeslot t on day h of the planning horizon, $y_{p,s,i,r,t,h} = 0$, otherwise.
y:	Vector of $y_{p,s,i,r,t,h}$'s.
$w_{p,s,i,r,t,h}$:	$w_{p,s,i,r,t,h} = 1$, if resource r of type i for step s of CHP p starts the assignment at timeslot t on day h of CHP calendar,$w_{p,s,i,r,t,h} = 0$, otherwise.
w:	Vector of $w_{p,s,i,r,t,h}$'s.

Second-Stage Sets

Ω:	Set of outcomes or scenarios ω, where ω is an outcome of a multivariate random variable $\tilde{\omega}$ that describes resource availability and is defined on a probability space.
$\mathcal{D}^{\omega}(p)$:	Subset of CHP starting days in the planning horizon on which CHP p can start under scenario ω, indexed d^{ω}.
$\bar{\mathcal{D}}^{\omega}(p, d^{\omega})$:	Set of CHP calendar days for all steps of CHP p starting on day $d^{\omega} \in \mathcal{D}^{\omega}(p)$, indexed $\bar{h}$.

Second-Stage Parameters

$a^{\omega}_{p,s,i,r,t,\bar{h}}$:	$a^{\omega}_{p,s,i,r,t,\bar{h}} = 1$, if resource r of type i is available for step s of CHP p at start timeslot t on day $\bar{h}$ of CHP calendar under scenario ω, $a^{\omega}_{p,s,i,r,t,\bar{h}} = 0$, otherwise.
$b^{\omega}_{i,r,\bar{h}}$:	$b^{\omega}_{i,r,\bar{h}}$ is the total number of timeslots that resource r of type i is already assigned on day $\bar{h}$ when schedule under scenario ω.

Second-Stage Variables

$z_{\bar{d}}^{\omega}$:	$z_{\bar{d}}^{\omega} = 1$, if client starts the first appointment on day $\bar{d}$ of the planning horizon under scenario ω, $z_{\bar{d}}^{\omega} = 0$, otherwise.
z^{ω}:	$z^{\omega} = 1$, if cannot find feasible schedule starting on day $\bar{d}$, $z^{\omega} = 0$ otherwise.
$x_{p,s,i,r,\bar{h}}^{\omega}$:	$x_{p,s,i,r,\bar{h}}^{\omega} = 1$, if resource r of resource type i is assigned to step s of CHP p on day $\bar{h}$ under scenario ω, $x_{p,s,i,r,\bar{h}}^{\omega} = 0$, otherwise.
x^{ω}:	Vector of $x_{p,s,i,r,\bar{h}}^{\omega}$'s.
$y_{p,s,i,r,t,\bar{h}}^{\omega}$:	$y_{p,s,i,r,t,\bar{h}}^{\omega} = 1$, if resource r of type i required for step s of CHP p is assigned to timeslot t on day $\bar{h}$ of the planning horizon under scenario ω. $y_{p,s,i,r,t,\bar{h}}^{\omega} = 0$, otherwise.
y^{ω}:	Vector of $y_{p,s,i,r,t,\bar{h}}^{\omega}$'s.
$w_{p,s,i,r,t,\bar{h}}^{\omega}$:	$w_{p,s,i,r,t,\bar{h}} = 1$, if resource r of type i for step s of CHP p starts the assignment at timeslot t on day $\bar{h}$ of CHP calendar under scenario ω, $w_{p,s,i,r,t,h}^{c} = 0$, otherwise.
w^{ω}:	Vector of $w_{p,s,i,r,t,\bar{h}}^{\omega}$'s.
$L_{i,\bar{h}}^{min,\omega}$:	$L_{i,\bar{h}}^{min,\omega}$, is the minimum number of timeslots that resource type i is assigned on day $\bar{h}$ under scenario ω.
$L^{min,\omega}$:	Vector of $L_{i,\bar{h}}^{min,\omega}$'s.
$L_{i,\bar{h}}^{max,\omega}$:	$L_{i,\bar{h}}^{max,\omega}$, is the maximum number of timeslots that resource type i is assigned on day $\bar{h}$ under scenario ω.
$L^{max,\omega}$:	Vector of $L_{i,\bar{h}}^{min,\omega}$'s.

We are now ready to derive the SP scheduling model using the given notation. As mentioned earlier, a CHP typically involves multiple types of resources in some given step. For a CHP p, if $|\mathcal{I}(p,s)| = 1$ it means that only one resource type is needed in step s of the pathway. If $|\mathcal{I}(p,s)| \geq 2$ it means that more than two types of resources are required in step s. Based on the pathways we consider in this work, we shall restrict ourselves to no more than three resource types in a given

step. Therefore, let us index the resources by i_1, i_2, i_3, in that order. Since the resources are required to perform a given task in a particular sequence (including concurrently), we shall refer to this sequence as the resource *precedence order*. We denote the resource precedence order for CHP p and step s by $\mathcal{O}(p, s)$. Each element, $0, 1$, or 2 of $\mathcal{O}(p, s)$ will represent the sequence order. If a single resource type is needed in step s of CHP p, the sequence order will be written as $\mathcal{O}(p, s) = \{0\}$. If two resource types are need, the precedence order can be $\mathcal{O}(p, s) = \{0, 0\}$ or $\mathcal{O}(p, s) = \{0, 1\}$. The precedence order $\mathcal{O}(p, s) = \{0, 0\}$ means that step s of CHP p requires two resource types, i_1 and i_2, concurrently. When $\mathcal{O}(p, s) = \{0, 1\}$ it means that two resource types i_1 and i_2 are required, with the first resource being available before the second to complete the task. Notice that the $|\mathcal{O}(p, s)|$ is equal to the number of resources required in step s.

If three resources are required for step s, then the following three precedence orders are possible: $\mathcal{O}(p, s) = \{0, 0, 1\}$, $\mathcal{O}(p, s) = \{0, 1, 1\}$ and $\mathcal{O}(p, s) = \{0, 1, 2\}$. Precedence order $\mathcal{O}(p, s) = \{0, 0, 1\}$ means that resource type i_1 must be available at the same time as resource type i_2 and that resource types i_1 and i_2 must be available before resource type i_3. If the precedence order is $\mathcal{O}(p, s) = \{0, 1, 1\}$, it means that resource type i_1 must be available before i_2 and i_3, while resource types i_2 and i_3 must be available at the same time. If three resource types must be available one after the next, then we denote the precedence order as $\mathcal{O}(p, s) = \{0, 1, 2\}$. The six possible resource precedence orders required in a given step that we consider in thus study are listed Table 4.4.

Case	# Resources	$\mathcal{O}(p, s)$
0	$\lvert\mathcal{I}(p, s)\rvert = 1$	$\{0\}$
1	$\lvert\mathcal{I}(p, s)\rvert = 2$	{0,0}
2	$\lvert\mathcal{I}(p, s)\rvert = 2$	{0,1}
3	$\lvert\mathcal{I}(p, s)\rvert = 3$	{0,0,1}
4	$\lvert\mathcal{I}(p, s)\rvert = 3$	{0,1,1}
5	$\lvert\mathcal{I}(p, s)\rvert = 3$	{0,1,2}

Table 4.4: Six resource precedence order cases

In the two-stage SP model, we want to determine here-and-now (first-stage) the client's schedule for all the appointments in their CHP, while accounting for future uncertainty in the resources' availability required to complete the CHP. For a given client, the first-stage decision variable vector v specifies each resource's schedule, i.e., days and corresponding timeslots the resource is assigned to each step of the CHP, as well as the start timeslot on each day in the schedule. The first-stage objective is to minimize the total waiting time from the time of a pathway appointment request to when the client is first seen, referred to as *access time*. We want to reduce this access time while taking into account the resources' unknown availability in the future. Thus, given the first-stage decision v, the second-stage objective is to minimize expected future cost associated with workload balancing based on the resources' uncertain availability.

Mathematically, the objective can be written as follows:

$$\underset{z,x,y,w}{\text{Min}} \sum_{d \in \mathcal{D}(p)} c_d z_d + \mathbb{E}[f(z, \tilde{\omega})]. \tag{4.1}$$

The first term of the objective function (4.1) computes the time (in terms of days) from when a client request for a pathway appointment is made to when the client start their first appointment over the planning horizon. The scalar c_d is a cost factor, with higher values indicating that we want to schedule the client as soon as possible. We can vary the trade-off between client waiting time and expected resource workload balance simply by changing the value of c_d.

Given a first-stage decision (z, x, y, w) and outcome $\omega \in \Omega$ of ω of $\tilde{\omega}$, the second term is the (second-stage) expected recourse function and it calculates the expected sum of workload differences among resources of the same type to effect equity. We will give an explicit mathematical expression of the recourse function $f(z, \omega)$ later. Next, we define the first-stage constraints. Given the subset of days in the planning horizon on which CHP p can start, $\mathcal{D}(p)$, the following constraint selects one possible starting day from the earliest possible days:

$$\sum_{d \in \mathcal{D}(p)} z_d = 1. \tag{4.2}$$

To ensure that the needed resource r of type i to perform step s of CHP $p \in \mathcal{P}$ is selected on day d, we impose the constraint:

$$-z_d + \sum_{r \in \mathcal{R}(i)} x_{p,s,i,r,h} = 0, \ \forall s \in \mathcal{S}(p), i \in \mathcal{I}(p,s), d \in \mathcal{D}(p), h \in \bar{\mathcal{D}}(p,d). \tag{4.3}$$

The next constraint ensures that the required resources are assigned to a timeslot:

$$\begin{aligned} n_{p,s,i} \cdot x_{p,s,i,r,h} - \sum_{t \in \mathcal{T}} y_{p,s,i,r,t,h} = 0, \ \forall s \in \mathcal{S}(p), i \in \mathcal{I}(p,s), \\ r \in \mathcal{R}(i), d \in \mathcal{D}(p), h \in \bar{\mathcal{D}}(p,d). \end{aligned} \tag{4.4}$$

To choose a starting timeslot for the needed resource, the constraint below is added:

$$\begin{aligned} z_d - \sum_{t \in \mathcal{T}} \sum_{r \in \mathcal{R}(i)} w_{p,s,i,r,t,h} = 0, \ \forall s \in \mathcal{S}(p), i \in \mathcal{I}(p,s), d \in \mathcal{D}(d), \\ h \in \bar{\mathcal{D}}(p,d). \end{aligned} \tag{4.5}$$

The following constraint ensures that the resource is assigned to an activity only when the resource is available:

$$\begin{aligned} y_{p,s,i,r,t,h} \leq a_{p,s,i,r,t,h}, \ \forall s \in \mathcal{S}(p), i \in \mathcal{I}(p,s), r \in \mathcal{R}(i), \\ t \in \{1, ..., |\mathcal{T}|\}, d \in \mathcal{D}(d), h \in \bar{\mathcal{D}}(p,d). \end{aligned} \tag{4.6}$$

We impose the following constraint to guarantee that consecutive timeslots are selected if step s of

CHP p using resource r of type i requires more than one timeslot:

$$\sum_{t=t'}^{t'+n_{p,s,i}-1} y_{p,s,i,r,t,h} - n_{p,s,i} \cdot w_{p,s,i,r,t',h} \geq 0, \ \forall s \in \mathcal{S}(p), i \in \mathcal{I}(p,s), \\ r \in \mathcal{R}(i), t' \in \{1, ...|\mathcal{T}| - n_{p,s,i} + 1\}, d \in \mathcal{D}(p), h \in \bar{\mathcal{D}}(p,d). \tag{4.7}$$

Resource Precedence Order

When multiple resources are involved in a step of a CHP, we add the appropriate precedence order constraints for each given case. We refer to the list of the possible precedence order cases in Table 4.4 to ensure that each task in a CHP is assigned the needed resources in the required order:

Case 0: $|\mathcal{I}(p,s)| = 1$ *for step* s*, precedence order* $\mathcal{O}(p,s) = \{0\}$: No additional constraints are needed.

Case 1: $|\mathcal{I}(p,s)| = 2$ *for step* s *with resources indexed* i_1 *and* i_2*, precedence order* $\mathcal{O}(p,s) = \{0,0\}$.

$$w_{p,s,i_1,r_1,t,h} = \sum_{r_2 \in \mathcal{R}(i_2)} w_{p,s,i_2,r_2,t,h}, \ \forall \, i_1, i_2 \in \mathcal{I}(p,s), r_1 \in \mathcal{R}(i_1), \\ t \in \{1, ...|\mathcal{T}| - n_{p,s,i_1} + 1\}, d \in \mathcal{D}(d), h \in \bar{\mathcal{D}}(p,d). \tag{4.8a}$$

$$w_{p,s,i_1,r_1,t,h} = \sum_{r_2 \in \mathcal{R}(i_2)} w_{p,s,i_2,r_2,t,h}, \ r_1 \in \mathcal{R}(i_1), \\ t \in \{1, ...|\mathcal{T}| - n_{p,s,i_1} + 1\}, d \in \mathcal{D}(d), h \in \bar{\mathcal{D}}(p,d). \tag{4.8b}$$

Case 2: $|\mathcal{I}(p,s)| = 2$ *for step* s *with resources indexed* i_1 *and* i_2*, precedence order* $\mathcal{O}(p,s) = \{0,1\}$. Resource type i_1 must be available before i_2. In this case, we need to include the following

constraints for step s:

$$\begin{aligned} w_{p,s,i_1,r_1,t,h} \leq & \sum_{t'=t+n_{p,s,i_1}}^{|\mathcal{T}|-n_{p,s,i_2}+1} \sum_{r_2 \in \mathcal{R}(i_2)} w_{p,s,i_2,r_2,t',h}, \ \forall\, i_1, i_2 \in \mathcal{I}(p,s), \\ & r_1 \in \mathcal{R}(i_1), t \in \{n_{p,s,i_1}+1, ..., |\mathcal{T}| - n_{p,s,i_1} - n_{p,s,i_2}+1\}, \\ & d \in \mathcal{D}(d), h \in \bar{\mathcal{D}}(p,d). \end{aligned} \tag{4.9}$$

Case 3: $|\mathcal{I}(p,s)| = 3$ *for some step* s *with resources indexed* i_1*,* i_2 *and* i_3*, precedence order* $\mathcal{O}(p,s) = \{0,0,1\}$. Resource type i_1 and i_2 must be available at the same time before resource type i_3. In this case, we need to impose the following constraints for step s:

$$\begin{aligned} w_{p,s,i_1,r_1,t,h} = & \sum_{r_2 \in \mathcal{R}(i_2)} w_{p,s,i_2,r_2,t,h}, \ \forall i_1, i_2 \in \mathcal{I}(p,s), r_1 \in \mathcal{R}(i_1), \\ & t \in \{1, ...|\mathcal{T}| - n_{p,s,i_1} - n_{p,s,i_2}+1\}, d \in \mathcal{D}(d), h \in \bar{\mathcal{D}}(p,d). \end{aligned} \tag{4.10a}$$

$$\begin{aligned} w_{p,s,i_2,r_2,t,h} \leq & \sum_{t'=t+n_{p,s,i_2}}^{|\mathcal{T}|-n_{p,s,i_3}+1} \sum_{r_3 \in \mathcal{R}(i_3)} w_{p,s,i_3,r_3,t',h}, \ \forall i_2, i_3 \in \mathcal{I}(p,s), \\ & i_2 \neq i_3, r_2 \in \mathcal{R}(i_2), t \in \{n_{p,s,i_1}+1, ..., |\mathcal{T}| - n_{p,s,i_3}+1\}, \\ & d \in \mathcal{D}(d), h \in \bar{\mathcal{D}}(p,d). \end{aligned} \tag{4.10b}$$

Case 4: $|\mathcal{I}(p,s)| = 3$ *for some step* s *with resources indexed* i_1*,* i_2 *and* i_3*, precedence order* $\mathcal{O}(p,s) = \{0,1,1\}$. Resource type i_1 must be available before resource types i_2 and i_3, and resource types i_2 and i_3 must be available at the same time. In this case, we need to include the

following constraints for step s:

$$w_{p,s,i_1,r_1,t,h} \leq \sum_{t'=t+n_{p,s,i_1}}^{|\mathcal{T}|-n_{p,s,i_2}+1} \sum_{r_2 \in \mathcal{R}(i_2)} w_{p,s,i_2,r_2,t',h}, \ \forall i_1, i_2 \in \mathcal{I}(p,s),$$
$$r_1 \in \mathcal{R}(i_1), t \in \{1, ..., |\mathcal{T}| - n_{p,s,i_1} - n_{p,s,i_2} + 1\}, d \in \mathcal{D}(d),$$
$$h \in \bar{\mathcal{D}}(p,d). \tag{4.11a}$$

$$w_{p,s,i_2,r_2,t,h} = \sum_{r_3 \in \mathcal{R}(i_3)} w_{p,s,i_3,r_3,t,h}, \ \forall \ i_2 \neq i_3, i_2 \in \mathcal{I}(p,s),$$
$$t \in \{n_{n,p,s,i_1} + 1, ...|\mathcal{T}| - n_{p,s,i_2} + 1\}, d \in \mathcal{D}(d), h \in \bar{\mathcal{D}}(p,d). \tag{4.11b}$$

Case 5: $|\mathcal{I}(p,s)| = 3$ *for some step* s *with resources indexed* i_1*,* i_2 *and* i_3*, precedence order* $\mathcal{O}(p,s) = \{0,1,2\}$. Resource type i_1 must be available before resource type i_2, and resource type i_2 must be available before resource type i_3. In this case, the following constraints are added for step s:

$$w_{p,s,i_1,r_1,t,h} \leq \sum_{t'=t+n_{p,s,i_1}}^{|\mathcal{T}|-n_{p,s,i_2}-n_{p,s,i_3}+1} \sum_{r_2 \in \mathcal{R}(i_2)} w_{p,s,i_2,r_2,t',h}, \ \forall i_1, i_2 \in \mathcal{I}(p,s),$$
$$r_1 \in \mathcal{R}(i_1) t \in \{1, ..., |\mathcal{T}| - n_{p,s,i_1} - n_{p,s,i_2} - n_{p,s,i_3} + 1\},$$
$$d \in \mathcal{D}(d), h \in \bar{\mathcal{D}}(p,d). \tag{4.12a}$$

$$w_{p,s,i_2,r_2,t,h} \leq \sum_{t'=t+n_{p,s,i_2}}^{|\mathcal{T}|-n_{p,s,i_3}+1} \sum_{r_3 \in \mathcal{R}(i_3)} w_{p,s,i_3,r_3,t',h}, \ \forall i_2, i_3 \in \mathcal{I}(p,s),$$
$$i_2 \neq i_3, r_2 \in \mathcal{R}(i_2), t \in \{n_{p,s,i_1} + 1, ..., |\mathcal{T}| - n_{p,s,i_2} - n_{p,s,i_3} + 1\},$$
$$h \in \bar{\mathcal{D}}(p,d). \tag{4.12b}$$

When there are multiple resources involved in a step, the appropriate precedence order constraints given above have to be added to the formulation. For example, in the Insurance CHP (Figure 4.2), step 3 requires resources types OTW (Outreach Worker), EDU (Educator) and TRL (Training Location) with precedence order $\mathcal{O}(p,s) = \{0,1,1\}$. Therefore, precedence order Case

4 in Table 4.4 applicable and constraints (4.11a)-(4.11b) must be included in the formulation.

Tightening Constraints

The purpose of tightening a formulation in integer programming is to reduce the size of the problem and to speed up computation time. In Table 4.4, we specified resource precedence order cases and defined the constraints for each. When multiple resources are involved in a step of the CHP, the resources' *earliest* and *latest* assigned timeslots and start times can be determined. Using this observation, we can update constraints (4.4) - (4.7) to get a tighter formulation by setting the appropriate timeslot bounds within which an activity in a given step can occur. We should point out that in Case 1 when the precedence order is $\mathcal{O}(p,s) = \{0,0\}$, the two resources have to be available at the same time, thus the bound on assigned and start times is the same as for a single resource. Therefore, in this case we cannot tighten the formulation. However, for the other cases involving multiple resource types, we can update some of the constraints to eliminate redundant variables and constraints.

For resource type i (in precedence order), let the *earliest* assigned timeslot be denoted EA_i and the *latest* assigned timeslot be denoted LA_i. Similarly, let ES_i and LS_i denote the earliest and latest start time, respectively. Then appropriate values of EA_i, LA_i, ES_i and LS_i for each of the cases for a given i can be given as shown in Table 4.5.

Using the specifications in Table 4.5, we can tighten the formulation by updating constraints (4.4) - (4.7) using EA_i, LA_i, ES_i and LS_i as follows:

$$n_{p,s,i} \cdot x_{p,s,i,r,h} - \sum_{t=ES_i}^{LS_i} y_{p,s,i,r,t,h} = 0, \ \forall s \in \mathcal{S}(p), i \in \mathcal{I}(p,s), \\ r \in \mathcal{R}(i), d \in \mathcal{D}(p), h \in \bar{\mathcal{D}}(p,d). \tag{4.13}$$

i	EA_i	LA_i	ES_i	LS_i
			Case 2	
1	1	$\lvert\mathcal{T}\rvert - n_{p,s,i_2}$	1	$\lvert\mathcal{T}\rvert - n_{p,s,i_1} - n_{p,s,i_2} + 1$
2	$n_{p,s,i_1} + 1$	$\lvert\mathcal{T}\rvert$	$n_{p,s,i_1} + 1$	$\lvert\mathcal{T}\rvert - n_{p,s,i_2} + 1$
			Case 3	
1	1	$\lvert\mathcal{T}\rvert - n_{p,s,i_3}$	1	$\lvert\mathcal{T}\rvert - n_{p,s,i_1} - n_{p,s,i_3} + 1$
2	1	$\lvert\mathcal{T}\rvert - n_{p,s,i_3}$	1	$\lvert\mathcal{T}\rvert - n_{p,s,i_1} - n_{p,s,i_3} + 1$
3	$n_{p,s,i_1} + 1$	$\lvert\mathcal{T}\rvert$	$n_{p,s,i_1} + 1$	$\lvert\mathcal{T}\rvert - n_{p,s,i_3} + 1$
			Case 4	
1	1	$\lvert\mathcal{T}\rvert - n_{p,s,i_3}$	1	$\lvert\mathcal{T}\rvert - n_{p,s,i_1} - n_{p,s,i_3} + 1$
2	$n_{p,s,i_1} + 1$	$\lvert\mathcal{T}\rvert$	$n_{p,s,i_1} + 1$	$\lvert\mathcal{T}\rvert - n_{p,s,i_2} + 1$
3	$n_{p,s,i_1} + 1$	$\lvert\mathcal{T}\rvert$	$n_{p,s,i_1} + 1$	$\lvert\mathcal{T}\rvert - n_{p,s,i_3} + 1$
			Case 5	
1	1	$\lvert\mathcal{T}\rvert - n_{p,s,i_2} - n_{p,s,i_3}$	1	$\lvert\mathcal{T}\rvert - n_{p,s,i_1}$ $-n_{p,s,i_2} - n_{p,s,i_3} + 1$
2	$n_{p,s,i_1} + 1$	$\lvert\mathcal{T}\rvert - n_{p,s,i_3}$	$n_{p,s,i_1} + 1$	$\lvert\mathcal{T}\rvert - n_{p,s,i_2} - n_{p,s,i_3} + 1$
3	$n_{p,s,i_1} + n_{p,s,i_2}$ $+1$	$\lvert\mathcal{T}\rvert$	$n_{p,s,i_1} + n_{p,s,i_1}$ $+1$	$\lvert\mathcal{T}\rvert - n_{p,s,i_3} + 1$

Table 4.5: Timeslot bounds for each case involving multiple resource types

$$z_d - \sum_{t=ES_i}^{LS_i} \sum_{r \in \mathcal{R}(i)} w_{p,s,i,r,t,h} = 0, \ \forall s \in \mathcal{S}(p), i \in \mathcal{I}(p,s), d \in \mathcal{D}(d), \\ h \in \bar{\mathcal{D}}(p,d). \tag{4.14}$$

$$y_{p,s,i,r,t,h} \leq a_{p,s,i,r,t,h}, \ \forall s \in \mathcal{S}(p), i \in \mathcal{I}(p,s), r \in \mathcal{R}(i), \\ t \in \{EA_i, ..., LA_i\}, d \in \mathcal{D}(d), h \in \bar{\mathcal{D}}(p,d). \tag{4.15}$$

$$\sum_{t=t'}^{t'+n_{p,s,i}-1} y_{p,s,i,r,t,h} - n_{p,s,i} \cdot w_{p,s,i,r,t',h} \geq 0, \ \forall s \in \mathcal{S}(p), i \in \mathcal{I}(p,s), \\ r \in \mathcal{R}(i), t' \in \{ES_i, ..., LS_i\}, d \in \mathcal{D}(p), h \in \bar{\mathcal{D}}(p,d). \tag{4.16}$$

Complete Formulation

Putting everything together, the two-stage SP pathway scheduling model can be given as follows:

$$\underset{z,x,y,w}{\text{Min}} \sum_{d \in \mathcal{D}(p)} c_d z_d + \mathbb{E}[f(z, \tilde{\omega})] \tag{4.17}$$

$$\text{s.t. } Constraints \text{ (4.2)} - \text{(4.3)}$$

$$Constraints \text{ (4.8)} - \text{(4.12)} \; needed \; for \; the \; CHP$$

$$Constraints \text{ (4.13)} - \text{(4.16)}$$

$$z_d \in \{0,1\}, \forall d \in \mathcal{D}(p), x_{p,s,i,r,h},\ y_{p,s,i,r,t,h},\ w_{p,s,i,r,t,h} \in \{0,1\},$$

$$\forall p \in \mathcal{P}, s \in \mathcal{S}(p), i \in \mathcal{I}(p,s), r \in \mathcal{R}(i), t \in \mathcal{T}, h \in \bar{\mathcal{D}}(p,d).$$

The recourse function $f(z, \omega)$ computes the future cost based on the first-stage schedule defined by z (start date) and an outcome (scenario) ω of $\tilde{\omega}$. The scenario ω reveals the future resource availability for all steps of the CHP under consideration in the second-stage. Thus, uncertainty is resolved in the second-stage and we need to find and assign resources to the schedule z for every day and step of the CHP, while optimizing the workload balance. For a given (z, ω), the recourse function $f(z, \omega)$ can be given explicitly as the value function of the following subproblem:

$$f(z,\omega) = \underset{z^\omega, z^\omega_{\bar{d}}, x^\omega, y^\omega, w^\omega, L^{min,\omega}, L^{max,\omega}}{\text{Min}} \sum_{i \in \mathcal{I}(p)} \sum_{\bar{h} \in \mathcal{D}(p,d^\omega)} (L^{max,\omega}_{i,\bar{h}} - L^{min,\omega}_{i,\bar{h}}) + M z^\omega \tag{4.18a}$$

$$\text{s.t. } z^\omega_{\bar{d}} + z^\omega = 1,\ \bar{d} = d \mid z_d = 1,\ d \in \mathcal{D}(p) \tag{4.18b}$$

$$- z^\omega_{\bar{d}} + \sum_{r \in \mathcal{R}(i)} x^\omega_{p,s,i,r,\bar{h}} = 0,\ \forall s \in \mathcal{S}(p), i \in \mathcal{I}(p,s), \bar{h} \in \mathcal{D}(p,\bar{d}),$$

$$\bar{d} = d \mid z_d = 1,\ d \in \mathcal{D}(p) \tag{4.18c}$$

$$n_{p,s,i} \cdot x^\omega_{p,s,i,r,\bar{h}} - \sum_{t=EA_i}^{LA_i} y^\omega_{p,s,i,r,t,\bar{h}} = 0,\ \forall s \in \mathcal{S}(p), i \in \mathcal{I}(p,s), r \in \mathcal{R}(i),$$

$$\bar{h} \in \mathcal{D}(p,\bar{d}),\ \bar{d} = d \mid z_d = 1,\ d \in \mathcal{D}(p) \tag{4.18d}$$

$$z^\omega_{\bar{d}} - \sum_{t=ES_i}^{LS_i} \sum_{r=1}^{|\mathcal{R}(i)|} w^\omega_{p,s,i,r,t,\bar{h}} = 0,\ \forall s \in \mathcal{S}(p), i \in \mathcal{I}(p,s), \bar{h} \in \mathcal{D}(p,\bar{d}),$$

$$t \in \{ES_i, ..., LS_i\},\ \bar{d} = d \mid z_d = 1,\ d \in \mathcal{D}(p) \tag{4.18e}$$

$$- y^\omega_{p,s,i,r,t,\bar{h}} \geq -a^\omega_{p,s,i,r,t,\bar{h}},\ \forall s \in \mathcal{S}(p), i \in \mathcal{I}(p,s), r \in \mathcal{R}(i),$$

$$t \in \{EA_i, ..., LA_i\}, \bar{h} \in \mathcal{D}(p,\bar{d}),\ \bar{d} = d \mid z_d = 1,\ d \in \mathcal{D}(p) \tag{4.18f}$$

$$\sum_{t=t'}^{t'+n_{p,s,i}-1} y^\omega_{p,s,i,r,t,\bar{h}} - n_{p,s,i} \cdot w^\omega_{p,s,i,r,t'\bar{h}} \geq 0,\ \forall s \in \mathcal{S}(p), i \in \mathcal{I}(p,s),$$

$$r \in \mathcal{R}(i), t' \in \{ES_i, ..., LS_i\}, \bar{h} \in \mathcal{D}(p,\bar{d}), \bar{d} = d \mid z_d = 1,\ d \in \mathcal{D}(p) \tag{4.18g}$$

$$L^{max,\omega}_{i,\bar{h}} - \sum_{t=EA_i}^{LA_i} y^\omega_{p,s,i,r,t,\bar{h}} \geq b^\omega_{i,r\bar{h}}, \forall s \in \mathcal{S}(p), i \in \mathcal{I}(p,s), r \in \mathcal{R}(i),$$

$$\bar{h} \in \mathcal{D}(p,\bar{d}),\ \bar{d} = d \mid z_d = 1,\ d \in \mathcal{D}(p) \tag{4.18h}$$

$$\tag{4.18i}$$

$$- L_{i,\bar{h}}^{min,\omega} + \sum_{t=EA_i}^{LA_i} y_{p,s,i,r,t,\bar{h}}^{\omega} \geq -b_{i,r,\bar{h}}^{\omega}, \forall s \in \mathcal{S}(p), i \in \mathcal{I}(p,s), r \in \mathcal{R}(i),$$

$$\bar{h} \in \mathcal{D}(p,\bar{d}),\ \bar{d} = d \mid z_d = 1,\ d \in \mathcal{D}(p) \tag{4.19a}$$

$$x_{p,s,i,r,\bar{h}}^{\omega} \in \{0,1\},\ y_{p,s,i,r,t,\bar{h}}^{\omega} \in \{0,1\},\ w_{p,s,i,r,t,\bar{h}}^{\omega} \in \{0,1\}, z_{\bar{d}}^{\omega} \in \{0,1\},$$

$$z^{\omega} \in \{0,1\}, L_{i,\bar{h}}^{max,\omega}, L_{i,\bar{h}}^{min,\omega} \geq 0, \forall p \in \mathcal{P}, s \in \mathcal{S}(p), i \in \mathcal{I}(p,s), r \in \mathcal{R}(i),$$

$$t \in \mathcal{T}, \bar{h} \in \mathcal{D}(p,\bar{d}), \bar{d} = d \mid z_d = 1,\ d \in \mathcal{D}(p). \tag{4.19b}$$

In objective of subproblem (4.18) we minimize the total difference between the maximum and minimum workload among resources of the same type to enable workload balancing. We add a sufficiently large penalty M ('big-M') to the second term of the objective function term to enforce *relatively complete recourse* by allowing z^{ω} to take a value of one when we cannot find a feasible schedule starting on day $\bar{d} = d \mid z_d = 1,\ d \in \mathcal{D}(p)$. This is enforced by constraint (4.18b). Combining constraints (4.18b)-(4.18g) ensures that given a first-stage schedule starting on day $\bar{d}$, we can find a schedule under scenario ω that starts on the day specified in the first-stage by decision z. Otherwise, $z^{\omega} = 1$, implying that we cannot find a schedule that is feasible for scenario ω due to some resources not being available. More specifically, constraints (4.18c) assigns resources needed to each step of the CHP for each day required in the CHP. Constraints (4.18d) allocate the number of consecutive timeslots needed for each step of the CHP for each day required in the pathway.

The start timeslot for each step of the CHP for each day required in the CHP is determined by constraints (4.18e), while each resource's availability for each timeslot is set using constraints (4.18f). Constraints (4.18g) assigns each resource available timeslots for each step of the CHP for each day required in the CHP. Constraints (4.18h) compute the maximum workload for each type of resource, while constraints (4.19a) compute the minimum workload. Finally, constraints (4.19b) enforce the binary and nonnegativity restrictions on the decision variables. This SP model was implemented and the CPLEX solver used to solve instances of the problems in a simulation

setting of a Pathways Community HUB. With 15-minute timeslots in an 8-hour day, the maximum difference between $L_{i,\bar{h}}^{max,\omega}$ and $L_{i,\bar{h}}^{min,\omega}$ is 32. Therefore, since the earliest starting day is desired, in our implementation we set the minimum value of c_d in the model to be 40. Next, we report the results of a computational study based on a simulation model for a real-setting to evaluate the performance of the SP approach.

4.4 Results

We first report computational results for all the three demand cases associated with client scheduling performance measures in Tables 4.6 and 4.7. Table 4.6 shows the results under the deterministic setting assuming known resource availability scenarios, whereas 4.7 shows the results for the stochastic settings. In the tables column 'NWB' lists the results for no workload balancing, while column 'WB' lists the results for workload balancing. The total of number of clients generated under NWB and WB for each case is the same as expected.

Table 4.6: Client waiting time results under the deterministic setting

	Case I		Case II		Case III	
Performance Measure	NWB	WB	NWB	WB	NWB	WB
Waiting time (days)	1.67	1.50	2.11	2.52	3.35	3.54
Total clients	747	747	1506	1506	2262	2262
Number of clients not scheduled	0.0	0.0	0.7	0.3	33.0	42.7
Number of clients have to wait	24	28	206	256	1041	1233

Table 4.7: Client waiting time results under the stochastic setting

	Case I		Case II		Case III	
Performance Measure	NWB	WB	NWB	WB	NWB	WB
Waiting time (days)	1.55	1.8	2.65	2.68	4.03	4.25
Total clients	738	738	1480	1480	2230	2230
Number of clients not scheduled	19.3	20.7	35	35	215	227
Number of clients have to wait	81.3	154	485	515	1529	1571

Under the deterministic setting, the results show that client waiting time is about 1.5 days for Case I, about 2.5 days for Case II, and about 3.5 days for Case III. This shows that increased client demand results in increased waiting time on average. However, for all the three demand cases workload balancing does not significantly affect waiting time, which is desirable. Under the stochastic setting, we see that client waiting time increases: about 2 days for Case I, about 3 days for Case II, and about 4 days for Case III. Comparing the deterministic versus the stochastic settings we can see that the deterministic setting gives optimistic results since different possible scenario realizations are not considered. Under both settings, however, we observe that increased client demand results in increased waiting time on average and that workload balancing does not significantly affect waiting time.

The number of clients that are *not* scheduled within 10 days due to resource unavailability is less under the deterministic setting compared to the stochastic setting. Again, this is because the deterministic setting assumes known resource availability, which in this case is optimistic resulting in fewer clients waiting. However, the stochastic setting takes a more pragmatic approach and gives results that are more realistic. Therefore, from hereon we will focus on the results for the stochastic setting.

We see that the number of clients that are *not* scheduled within 10 days due to resource unavailability almost doubles under Case II compared to Case I, and is almost about 11 times under Case III (about six times compared to Case II). This is an indication that client volume significantly affect schedules. Clearly, increased arrival while maintaining the same number of resources results in more clients not being scheduled. In fact, we see that more clients have to wait. Digging deeper into the results we found that most of the clients that are *not* scheduled are those assigned the Transportation CHP. One step of this CHP requires transportation time for 12 consecutive timeslots. To be able to schedule this CHP, we need to find a schedule with 12 consecutive available timeslots for all scenarios. Combining the number of scenarios and the consecutive timeslots requirement, the Transportation CHP has a higher chance of not being scheduled.

We also observed that among all the scheduled clients, about 20% have waiting time of about

two days for both NWB and NB approaches. Thus workload balancing provides a significant advantage since it does not adversely affect waiting time compared to no workload balancing. In terms of NWB versus WB, there is no significant impact on the number of clients that are *not* scheduled. However, we see a significant increase in the number of clients that have to wait. This is because workload balancing imposes equity (fairness) among the CHWs by requiring them to work similar number of timeslots. In turn this results in clients having to wait to be seen.

Computational results for resource utilization for the three demand cases are summarized in Table 4.8. The first column 'Res' lists the resource types, *Max, Mean* and *Min* represent maximum, average and minimum number of timeslots assigned to each resource. CV_{NWB} and CV_{WB} are the coefficients of variation for each resource type. The coefficient of variation is the ratio of the standard deviation to the mean and it shows the extent of variability in relation to the mean. The last column lists the ratio of the CV under NWB to that under WB. From the table we can see that the CV_{NWB} values are significantly higher than CV_{WB} values, an indication that workload balancing gives far less variability among the resource types, thus resulting in more equitable schedules. This is confirmed with the relatively large values of the ratio $\frac{CV_{NWB}}{CV_{WB}}$.

To glean further into the results, we include the plots for Case III showing the maximum and minimum timeslots that are assigned to the resources in Figure 4.4. The plots clearly show that the SP pathway scheduling model with workload balancing results in an equitable use of the resources. The average difference between maximum and minimum for no workload balancing is 319 timeslots, while that for workload balancing is about 40 timeslots. We can also clearly see which resource type is being 'overworked' the most. Resource PEC (Patient Counselor) stands out in all the three cases: without workload balancing one of the PEC works 959 timeslots while the other works only 102 timeslots. This means that one counselor is working eight times more than the other! With workload balancing, the difference is only 20 timeslots.

4.5 Discussion

The computational study reveals that the SP pathway scheduling model allow to optimally schedule clients in a Pathways Community HUB by minimizing client waiting time as well as

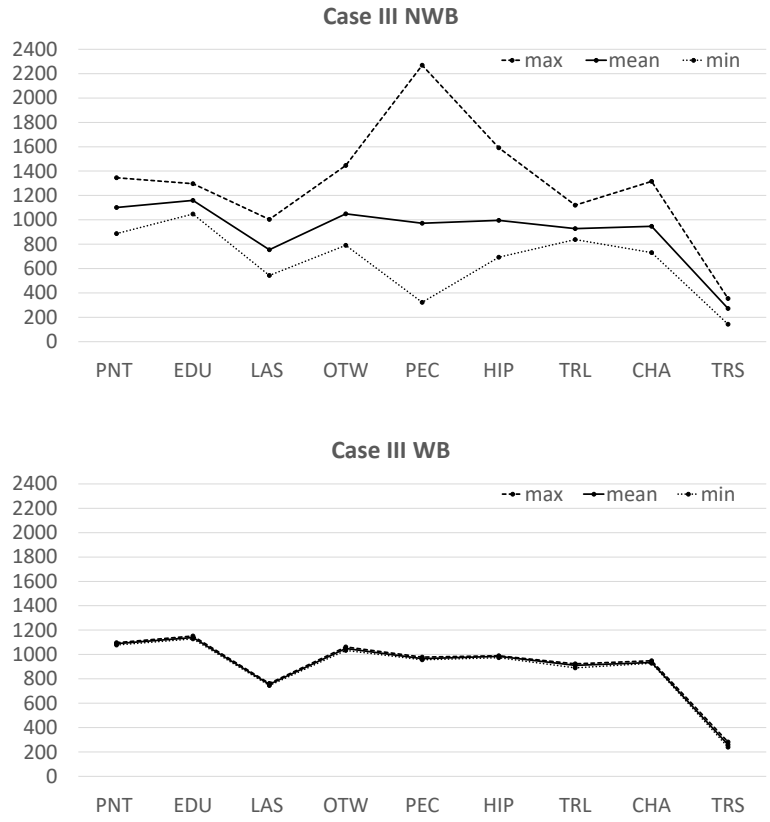

Figure 4.4: Resource utilization for Case III

Table 4.8: Computational results for resource utilization

	NWB				WB				
Res	Max	Mean (Time Slots)	Min	CV_{NWB}	Max	Mean (Time Slots)	Min	CV_{WB}	$\frac{CV_{NWB}}{CV_{WB}}$
Case I									
PNT	544.7	396.2	238.7	0.3274	409.3	396.2	383.7	0.0268	12.2
EDU	575	475.4	379	0.1694	515.3	475.4	444	0.0559	3.02
LAS	372	268	167.3	0.3137	275.3	268.1	261	0.0239	13.1
OTW	571	390.2	240	0.3406	405.3	390.2	376	0.0295	11.6
PEC	959	335.9	102.3	0.9417	352	335.9	321.3	0.0325	28.9
HIP	544.3	361.5	220	0.3758	373.3	361.5	344.3	0.0385	12.3
TRL	515.3	380.3	278.3	0.2230	407	380.3	365.3	0.0386	5.8
CHA	490.7	334.1	171.7	0.3970	355.3	334.1	312.7	0.0486	8.2
TRS	128	893.	40	0.4200	110	89	58	0.2540	1.7
Case II									
PNT	1095	800	609	0.2645	811	800	783	0.0152	17.4
EDU	1010	978.75	838	0.0878	532	526	523	0.0219	4.0
LAS	710	526	413	0.2495	789	783.5	774	0.0072	30.9
OTW	1121	783.5	502	0.2915	789	783.5	774	0.0072	40.2
PEC	2086	678.4	141	1.0610	689	678.6	671	0.0098	108.2
HIP	1251	721.5	390	0.4600	750	721.25	705	0.0239	19.2
TRL	868	743	678	0.1008	771	743	703	0.0306	3.3
CHA	905	659.5	459	0.3064	671	695.5	650	0.0123	24.8
TRS	276	200	114	0.3326	228	200	180	0.1020	3.3
Case III									
PNT	1345	1101	877	0.170915	1096	1088.7	1078	0.0071	24.1
EDU	1295	1101	887	0.0894	1151	1138.5	1128	0.0077	11.6
LAS	1003	754.7	543	0.2512	762	754.7	746	0.0087	28.7
OTW	1447	1049.25	791	0.238919	1062	1048.75	1033	0.0099	24.2
PEC	2269	972.2	323	0.7577	979	966.6	956	0.0097	78.5
HIP	1592	995.5	693	0.3551	990	984.5	974	0.0063	56.5
TRL	1121	927.6	838	0.1090	924	910.8	890	0.0129	8.4
CHA	1316	946.3	731	0.2383	948	935	928	0.0082	29.0
TRS	354	272	144	0.3371	282	260	240	0.0662	5.1

enabling workload balance among the CHWs. The results show that the MIP model can be optimistic depending on how the future resource availabilities are set. Therefore, we recommend to HUB managers to use the SP pathway scheduling model with workload balancing. This is because this model significantly reduces workload imbalance among the same resource types while providing the same amount of waiting time as the model with no workload balancing on average.

We should point out that the SP pathway scheduling model without workload balancing can create schedules that are disadvantageous to some CHWs. We saw for example, how one patient counselor (PEC) worked eight times more than another PEC. Clearly, this creates unfairness concerns for the HUB manager. Therefore, we recommend using workload balancing in order to get client schedules that are equitable in the use of limited resources in the Pathways Community HUB.

The proposed SP pathway scheduling model can also provide the HUB manager or scheduler a slew of useful information beyond the schedules and resource utilization. For example, by looking at the client wait time and/or resource utilization, the results of the model can provide guidance regarding which CHPs are being assigned the most and what resources are being utilized the most. This can help the HUB manager with making resource capacity expansion decisions.

Finally, even though we use timeslots in our models and results, knowing each CHW's hourly pay rate the manager can compute the cost associated with utilizing each CHW relative to both the assigned CHPs and the outcomes of the CHPs in terms of meeting the desired HUB objectives.

4.6 Conclusion

Scheduling and coordinating constrained resources in community healthcare settings at a centralized community level is challenging due to limited resources and the inherent dynamics of the processes and the organizational structures. Community health pathways (CHPs) have been introduced as a standardized interdisciplinary tool that details multiple steps of a healthcare-related service and the required resources for each step. However, the time window constraints for each step and the data uncertainty in resource availability makes this scheduling problem very challenging. On the other hand rising demand and costs of healthcare motivate the need for efficient schedules. In this work we developed an SP pathway scheduling model to schedule CHPs and community healthcare resources under resource availability uncertainty.

A computational study based on a real Pathways Community HUB setting provided several findings and managerial insights. The results show that the schedules provided by the deterministic model can be too optimistic and may not necessary work well under uncertainty in resource

availability. Client wait time depends on the client demand, with high demand resulting in longer waiting time. The study also shows that the workload balancing is preferred because it provides schedules with similar workloads across resources of the same type while providing waiting times that are comparable to when no workload balancing is applied. Managerial insights include the recommendation to HUB managers and schedulers to use workload balancing not only to minimize client waiting time, but also to guarantee client schedules that result in equitable use of limited resources in the Pathways Community HUB. Future work along this line of work include extending the SP pathway scheduling model to allow for resource capacity expansion decisions and budget constraints. There is also a need to develop a fast decomposition algorithm for the scheduling problem to speed up computation time.

5. OPTIMAL VACCINE ALLOCATION FOR COVID-19

COVID-19 caused by Severe Acute Respiratory Syndrome SARS-CoV-2 virus was declared a pandemic by the World Health Organization in early 2020. Despite concerted efforts by health authorities to contain the disease, the virus has continued to spread and mutate leading to new variants with uncertain transmission characteristics. Therefore, there is a need for new data-driven models for determining optimal vaccination policies that adapt to the new variants and uncertain vaccine efficacy. Motivated by this challenge, we derive an integrated chance constraints stochastic programming (ICC-SP) approach for finding optimal vaccination policies for epidemics that incorporates uncertain disease transmission characteristic and population demographics. An optimal vaccination policy specifies the proportion of individuals in a given household-type to vaccinate to bring the reproduction number to below one. The ICC-SP approach provides a quantitative alternative to qualitative chance constraints by allowing to bound the expected excess of a chance constraint by the largest acceptable amount according to the decision-maker's level of risk averseness. We derive a multi-community ICC-SP model to determine vaccination policies to control outbreaks under different risk levels. The model includes census demographics, vaccination status, age-related heterogeneity in disease susceptibility and infectivity, variants, and vaccine efficacy. The new methodology was tested on real data for seven neighboring counties in the U.S. state of Texas. The results are promising and show, among other findings, that vaccination policies for controlling an outbreak should prioritize vaccinating larger households as well as age groups with relatively high combined susceptibility and infectivity.

5.1 Introduction

The first outbreak of COronaVIrus Disease of 2019 (COVID-19) caused by Severe Acute Respiratory Syndrome Coron-2aVirus (SARS-CoV-2) was reported in December 2019. This highly contagious virus rapidly erupted, and three months later, the World Health Organization (WHO) termed the disease a pandemic. It is probably the most devastating pandemic in the last 100 years

after the Spanish flu. Despite the elaborate efforts by health officials to contain the disease, this virus spread to all regions of the world within only a few months. At the early stage of COVID-19 spreading, a variety of non-pharmaceutical interventions were implemented, such as border closures, restrictions on gathering, social distancing, quarantining, mask mandates, business closures, religious institutions and schools, travel restrictions and contact tracing. These mitigation interventions are intended to slow the community transmission of COVID-19.

The basic reproduction number, R_0, is one of the important measures of community transmission of infectious disease. R_0 is an epidemiological scale to measure the contagiousness of an infectious agent and it is defined as the the number of secondary infections caused by a primary case within a completely susceptible population in the absence of any deliberate intervention in disease transmission [59, 60]. The value of R_0 quantifies the transmissibility of an infectious disease at the initial stages of an epidemic and it helps the health authorities to understand the course of a disease transmission and to design various intervention strategies. However, in practice, a population will rarely be totally susceptible to an infection. Therefore, it is important to evaluate the time-dependent variation in transmissibility under the impact of mitigation interventions and decline in susceptible population [61]. This time-dependent variation is captured through the effective reproduction number R_t, which is defined as the average number of secondary infections caused by a primary case at time t [61, 62]. R_t suggests that an outbreak is under control if $R_t \leq 1$ and continue if the value is greater than 1.

Currently, three vaccines are authorized and recommended in the U.S.: Pfizer-BioNTech, Moderna, and Johnson & Johnson's Janssen [63]. Recent studies suggest that the currently authorized mRNA vaccines (Pfizer-BioNTech or Moderna) are highly effective against the ancestral strain and Alpha variant [64, 65]. Studies for Johnson & Johnson's Janssen are underway to learn more about the effectiveness against COVID-19. However, just influenza virus, SARS-CoV-2 virus keeps changing through mutation. Evidence shows that some of the new variants, such as the currently dominant Delta variant, can be more severe in terms of illness and transmissibility, and the vaccine may be less efficacious [5, 6]. As of 16 August, more than half of the population in the U.S. were

fully vaccinated against COVID-19 [66]. However, SARS-Cov-2 transmission is still at high levels in different regions of the U.S.. There is an urgent need for an effective vaccination strategy to compete with the variant mutation and fading vaccine efficacy.

5.2 Literature review

In epidemiology modeling, vaccination policies depending on varying factors have been widely studied. The approaches range from deterministic to stochastic, computer simulation to statistical prediction [40, 41, 42]. Bubar et al. apply a deterministic approach to evaluate the impact of vaccine efficacy, susceptibility, infectivity, and population variation on mortality, cumulative incidence, and years of life lost [67]. Manuel et al. investigate the consequences in hospitalization occupancy when varying the inter-dose interval [68]. Throughout their experiments, they explore the impact of vaccination strategies under different scenarios regarding efficacy, coverage, vaccine-induced, and natural immunity. Matrajt et al. compare vaccination strategies under different hypothetical vaccine efficacy [69]. These articles conduct a series of experiments under a broad range of scenarios in which a single parameter is varying. However, the essential and conclusive epidemiological characteristics of the virus, vaccine efficacy, vaccine-induced, and natural immunity remains under study, and their variations coexist [70]. Therefore, there is need of a stochastic model to account for multiple scenarios simultaneously. Given that a stochastic program seeks a feasible solution for all realizations of random parameters over a given objective or a solution that accepts a certain level of infeasibility.

In this chapter, we build on the stochastic programming framework developed by Tanner et al. [41]. The authors extend Becker et al. [71] deterministic optimal vaccine allocation model into a stochastic setting, assuming no one is vaccinated yet in a single community. Currently, about half of the population in the U.S. was already fully vaccinated against COVID-19 [72]. The assumption that no one is vaccinated yet is no longer valid for an optimal vaccination strategy. Therefore, we extend the work of Tanner et al. to consider a population with different vaccination statuses including age-related differences in susceptibility and infectivity and variant related transmissibility. We implement and test the new approach on data for a population center and its surrounding

communities with a sparse population. In general, the contagious disease has a higher likelihood to spread faster in a densely populated area due to the high number of social contacts [73]. The multi-community stochastic model suggests a vaccination strategy that can contain the outbreak for a set of communities as a whole rather than as individual entities.

The contributions include a new stochastic programming based methodology to determine the optimal vaccination policies to control the COVID-19 outbreak ($R_t \leq 1$) in a set of communities. This new methodology considers uncertainty in parameters such as human interactions, transmission characteristics, and vaccine efficacy towards different emerging COVID-19 variants. This stochastic model captures the socio-demographic variations including household types and vaccination status in the population. We conducted numerical experiments with different accepted risk levels, which can provide an evidence-based rationale for health authorities to make critical decisions. The accepted risk levels are often prescribed by health officials based on the historical severity of the pandemic. Currently, the Delta variant is actively soaring infection numbers, and CDC suggests moderately to severely immunocompromised individuals who are already fully vaccinated to get a booster shot. At the time of writing this chapter, the efficacy of the booster shot remains unknown [74]. Our setup allows to explore the optimal strategies for additional immunization with hypothetical efficacy to set the basis for possible future vaccination policies.

The rest of this chapter is organized as follows: We derive the new multi-community stochastic model for optimal vaccination strategies in the next section. in Section 5.4 we describe the model parameters and population datasets. We report the results of our computational study in Section 5.5. We end the chapter with a summary and future work in Section 5.6.

5.3 Multi-Community Stochastic Model

In this section, we consider a stochastic model for a population under different vaccination statuses, as well as discuss the demographic data and uncertain parameters used in the model. During epidemics, it is critical to understand both the course of the transmission path and the likely number of infections. A common approach to forecast the number of infections is to use epidemic compartmental models, such as the susceptible-exposed-infected-recovered (SEIR) model. The SEIR

model aims to predict the number of individuals who are susceptible to infection, are exposed, are actively infected, or have recovered from infection at any given time. In this section, we consider a model of disease transmission in a community based on the work of Becker and Starczak [71] and Tanner et al. [41]. Tanner et al. extended the deterministic model to the stochastic setting using chance-constrained approach, where the disease transmission parameters are uncertain. Both models consider a single community of households and assume that no one in the community is vaccinated yet. However, in this chapter we extend their approach to multiple communities with variations in vaccination status in a stochastic setting. An effective vaccination strategy aims to contain the outbreak by achieving herd immunity and bringing $R_t \leq 1$. The optimal solution gives the proportion of individuals under demographic variation that must be vaccinated to prevent epidemics. The optimal solution depends on the variants, household sizes, vaccine status, transmission characteristics of each variant. In epidemiology, the term vaccination coverage refers to the proportion of individuals who are vaccinated. In this work, we are interested in determining an optimal strategy that has a minimum vaccination coverage based on household size under variation in vaccination status to ensure that $R_t \leq 1$.

As mentioned in Section 5.1, R_t is the effective reproduction number, which refers to the average of secondary cases generated by an infected case during an infectious period. R_t does not assume a fully susceptible population and depends on the current immunity of the population [75]. In this chapter, we consider the post-vaccination reproduction number, denoted as R_{HVc}, which represents the effective reproduction number after vaccination in community c. The vaccination coverage required is to achieve $R_{HVc} \leq 1$ so that the herd immunity induced by vaccination is at a sufficiently high level to prevent epidemics.

Computing R_{HVc} requires several parameters, which cannot be represented by a single exact number. For example, vaccine efficacy, transmission rate, and individual contact rate, varies in a range following a particular distribution. Therefore, instead of the deterministic model using a point estimate, we consider a stochastic programming model that allows for the parameters to be random and characterized by discrete probability distributions. In addition, at the time of writing

this article, the U.S. suggested a booster shot for those who are already vaccinated. However, the booster vaccine-induced immunity and SARS-CoV-2 transmission capacity from a vaccinated individual remain unexplained, which has motivated us to explore how vaccination status affects the optimal vaccination allocation in our case studies. Due to the uncertainty of parameters, in some scenarios, it might be impossible to bring the post-vaccination reproduction number R_{HVc} below one. We impose an *integrated chance-constraint* (ICC) and a *chance-constrained* (CC) model over the set of constraints on those scenarios where R_{HVc} exceeds a value of one. In ICC model, the amount by how much those constraints are violated is bounded by a reliability level α_c. Mathematically, ICC is expressed as $\mathbb{E}[R_{HVc} - 1] \leq \alpha_c$, where $\mathbb{E}$ is the expectation over all scenarios in community c. In CC model, the probability of violated scenarios is bounded by γ_c, and mathematically it can be expressed as $\mathbb{P}\{R_{HVc} \leq 1\} \geq (1 - \gamma_c)$ Next, we define the notation we use in our mathematical models under heterogeneity in a population with different vaccination statuses.

Sets and Indices	
$\mathbb{C}$	Set of communities, element $c \in \mathbb{C}$.
$\mathbb{N}$	Set of household types, element $n \in \mathbb{N}$.
$\mathbb{K}$	Set of vaccination status, element $k \in \mathbb{K}$.
$\mathbb{I}$	Set of person age groups, element $i \in \mathbb{I}$.
$\mathbb{V}$	Set of vaccination policies, element $v \in \mathbb{V}$.
Ω_c	Set of outcomes (scenarios) for community $c \in \mathbb{C}$, element $\omega_c \in \Omega_c$.
Parameters	
$\tilde{\omega}_c$	Multivariate random variable (defined on a probability space) whose outcome is $\omega_c \in \Omega_c$; describes the uncertain parameters for R_{HVc}.
R_{HVc}	Post-vaccination reproduction number for community $c \in \mathbb{C}$.
$a_{nkvc}(\tilde{\omega}_c)$	Uncertain R_{HVc} parameter that captures the impact of vaccination policy $v \in \mathbb{V}$ in a type n household with vaccination status k in community $c \in \mathbb{C}$.
$m_c(\tilde{\omega}_c)$	Uncertain number of close contacts that an infective makes on average with persons from other household in the course of his/her infectious period in a community $c \in \mathbb{C}$.
H_{kc}	Number of households with vaccination status k in community $c \in \mathbb{C}$.
$p(n)$	Number of persons in a household of type n.
$f(n, v)$	Number of persons to vaccinate in a household size of n when vaccination policy $v \in \mathbb{V}$ is implemented.
h_{nkc}	Proportion of type n households with vaccination status k in community $c \in \mathbb{C}$.
μ_c	Average household size in a community, $\mu_c = \sum_{n \in \mathbb{N}} \sum_{k \in \mathbb{K}} p(n) h_{nkc}$.
$b(\tilde{\omega}_c)$	Uncertain transmission rate within a household.
$\beta_{kic}(\tilde{\omega}_c)$	Uncertain susceptibility for $i \in \mathbb{I}$ age group person with vaccination status $k \in \mathbb{K}$ in community $c \in \mathbb{C}$.

$\lambda_{kic}(\tilde{\omega}_c)$	Uncertain infectivity for $i \in \mathbb{I}$ age group person with vaccination status $k \in \mathbb{K}$ in community $c \in \mathbb{C}$.
$\epsilon_k(\tilde{\omega}_c)$	Uncertain vaccine efficacy towards population with vaccination status $k \in \mathbb{K}$.
Decision Variables	
x_{nkvc}	Proportion of n sized households with vaccination status k under vaccination policy $v \in \mathbb{V}$ implemented in community $c \in \mathbb{C}$.

We define the expression of R_{HVc} based on Becker and Starczak's model of disease spread [71]. R_{HVc} is defined in relation to $a_{nkvc}(\tilde{\omega_c})$, where $a_{nkvc}(\tilde{\omega_c})$ is a random variable depending on $\tilde{\omega}$. In this formulation, we consider two vaccination status. If the status index $k = 0$, it means that no one in that household is vaccinated, whereas $k = 1$ means that everyone in that household is vaccinated. Given x_{nkvc} is the proportion of n-sized households with vaccination status k in which vaccination policy v has been implemented, R_{HVc} for a community c is expressed as follows:

$$R_{HVc} = \sum_{n\in\mathbb{N}} \sum_{k\in\mathbb{K}} \sum_{v\in\mathbb{V}} a_{nkvc}(\tilde{\omega_c}) x_{nkvc}. \tag{5.1}$$

In this model, we assume that there are significant age and vaccination status related differences in the *susceptibility* and *infectivity* of individuals. To capture these differences, we define a set of groups of people $\mathbb{I}$ in which susceptibility and infectivity are differentiated by age. We denote the susceptibility and infectivity of group i with vaccination status k in community c by $\beta_{kic}(\tilde{\omega_c})$ and $\lambda_{kic}(\tilde{\omega_c})$ respectively. Here, We consider three age groups, A, B, and C, as follows: $A = (age \leq 19)$, $B = (20 \leq age \leq 64)$, and $C = (age \geq 65)$. The age groups can be expanded as need based on the age-difference related infectivity and susceptibility. For each household of type n, $p(n)$ represents the total number of members in the household. $p_i(n)$ denotes the number of members in group i for household type $p(n)$, where $i \in \{A, B, C\}$. The possible vaccination policies for a type n household are represented by $(f_A(n, v), f_B(n, v), f_C(n, v))$, the number of household members vaccinated in group A, B, and C, respectively. Table 5.1 gives an example illustration for $p(n)$ values of 1 and 2.

Given the proportion of type n household with v vaccinated members, x_{nkvc}, the post-vaccination

Household Type	Household Size	Household Composition	Total vaccination policies	Possible vaccination policies for a type n Household
n	$p(n)$	$(p_A(n),$ $p_B(n),$ $p_C(n))$	$(p_A(n)+1)$ $(p_B(n)+1)$ $(p_C(n)+1)$	$(f_A(n,v), f_B(n,v), f_C(n,v))$
1	1	(1, 0, 0)	2	(0, 0, 0), (1, 0, 0)
2	1	(0, 1, 0)	2	(0, 0, 0), (0, 1, 0)
3	1	(0, 0, 1)	2	(0, 0, 0), (0, 0, 1)
4	2	(2, 0, 0)	3	(0, 0, 0), (1, 0, 0), (2, 0, 0)
5	2	(0, 2, 0)	3	(0, 0, 0), (0, 1, 0), (0, 2, 0)
6	2	(0, 0, 2)	3	(0, 0, 0), (0, 0, 1), (0, 0, 2)
7	2	(1, 1, 0)	4	(0, 0, 0), (0, 1, 0), (1, 0, 0), (1, 1, 0)
8	2	(0, 1, 1)	4	(0, 0, 0), (0, 0, 1), (0, 1, 0), (0, 1, 1)
9	2	(1, 0, 1)	4	(0, 0, 0), (0, 0, 1), (1, 0, 0), (1, 0, 1)

Table 5.1: Example household types and vaccination policies under heterogeneous population for $p(n) = 1$ and $p(n) = 2$

reproduction number R_{HVc} for some community c is given by equation (5.1). Under the assumption of heterogeneity, the explicit expression for R_{HVc} considers the age-stratified groups. In Becker and Starczak's model [71], $a_{nkvc}(\tilde{\omega_c})$ is deterministic, assuming all the parameters are known. On the contrary, we model $a_{nkvc}(\tilde{\omega_c})$ as a random variable and the outcome (scenario) of $\tilde{\omega_c}$, ω_c is a *quintuple*: $\omega_c := \{m_c(\omega_c),\ b(\omega_c),\ \epsilon(\omega_c),\ \beta_{kc}(\omega_c),\ \lambda_{kc}(\omega_c)\}$. Consequently, this uncertain parameter can be defined as follows:

$$
\begin{aligned}
a_{nkvc}(\tilde{\omega_c}) =& \frac{m_c(\tilde{\omega_c})h_{nkc}}{\mu_c}\Big\{\sum_{i\in I}\beta_{kic}(\tilde{\omega_c})\lambda_{kic}(\tilde{\omega_c})[(1-b(\tilde{\omega_c}))(p_i(n)-f_i(n,v)\epsilon_k(\tilde{\omega_c}))+ \\
& b(\tilde{\omega_c})f_i(n,v)\epsilon_k(\tilde{\omega_c})(1-\epsilon_k(\tilde{\omega_c}))]+ \\
& b(\tilde{\omega_c})\sum_{i\in I}\sum_{r\in I}\beta_{kic}(\tilde{\omega_c})\lambda_{krc}(\tilde{\omega_c})(p_i(n)-f_i(n,v)\epsilon_k(\tilde{\omega_c}))(p_i(r)-f_i(n,r)\epsilon_k(\tilde{\omega_c}))\Big\}. \qquad (5.2)
\end{aligned}
$$

In the absence of effective and successful treatment for optimal COVID-19, vaccination seems to be the potential way to prevent this epidemic. Then the goal is to have $R_{HVc} = \sum_{n=1}^{N}\sum_{v\in\mathbb{V}} a_{nvc}(\tilde{\omega_c})x_{nvc} \leq 1$. In practice, however, there might be some extreme scenarios where the vaccines can not prevent the epidemic. For instance, if vaccine efficacy is not sufficiently large, $R_{HVc} > 1$. This means that constraint $R_{HVc} \leq 1$ is violated. Therefore, we use the CC and ICC approach to allow a certain level of infeasibility in constraints.

We now ready to define the minimum coverage problem with CC approach as follows:

$$\text{Min} \quad \sum_{n\in\mathbb{N}}\sum_{k\in\mathbb{K}}\sum_{v=0}^{p(n)}\sum_{c\in\mathbb{C}} f_i(n,v)h_{nkc}x_{nkvc} \tag{5.3a}$$

$$\text{s.t} \quad \mathbb{P}\{\sum_{n\in\mathbb{N}}\sum_{k\in\mathbb{K}}\sum_{v=0}^{p(n)} a_{nkvc}(\omega)x_{nkvc} \leq 1\} \geq \gamma_c,\ \forall c \in \mathbb{C} \tag{5.3b}$$

$$\sum_{v=0}^{n} x_{nkvc} = 1, \forall n \in N;\ k \in \mathbb{K};\ \forall c \in \mathbb{C} \tag{5.3c}$$

$$x_{nkvc} \geq 0, \forall v \in \{0,\cdots,p(n)\};\ n \in \mathbb{N};\ k \in \mathbb{K};\ \forall c \in \mathbb{C};\ \forall \omega \in \Omega \tag{5.3d}$$

The minimum vaccination coverage problem applying ICC approach is defined as follows:

$$\text{Min} \quad \sum_{n\in\mathbb{N}}\sum_{k\in\mathbb{K}}\sum_{v=0}^{p(n)}\sum_{c\in\mathbb{C}} f_i(n,v)h_{nkc}x_{nkvc} \tag{5.4a}$$

$$\text{s.t} \quad \sum_{n\in\mathbb{N}}\sum_{k\in\mathbb{K}}\sum_{v=0}^{p(n)} a_{nkvc}(\omega)x_{nkvc} - e_{\omega c} \leq 1,\ \forall c \in \mathbb{C};\ \forall \omega \in \Omega \tag{5.4b}$$

$$\sum_{\omega\in\Omega} p_\omega e_{\omega c} \leq \alpha_c, \forall c \in \mathbb{C} \tag{5.4c}$$

$$\sum_{v=0}^{n} x_{nkvc} = 1, \forall n \in N;\ k \in \mathbb{K};\ \forall c \in \mathbb{C} \tag{5.4d}$$

$$x_{nkvc}, e_{\omega c} \geq 0, \forall v \in \{0,\cdots,p(n)\};\ n \in \mathbb{N};\ k \in \mathbb{K};\ \forall c \in \mathbb{C};\ \forall \omega \in \Omega \tag{5.4e}$$

The objective function (5.4a) determines the minimum vaccination coverage across communities. $R_{HVc} = \sum_{n=1}^{N}\sum_{v\in\mathbb{V}} a_{nkvc}(\tilde{\omega_c})x_{nkvc} \leq 1$ is to prevent an epidemic for each community. Constraints (5.4b) and (5.4c) are comprised of the integrated chance constraints allowing $R_{HVc} \leq 1$ to be violated by $z(\tilde{\omega}c)$, and the expected violation $\mathbb{E}[z(\tilde{\omega}_c)]$ not to exceed α_c. Constraints (5.4d) determine the proportion of persons to vaccinate for each household size in each community. Finally, constraints (5.4e) are nonnegativity restrictions on decision variables.

5.4 Model Parameters

In this section, we present the uncertain parameters used in the model. The communities are characterized by the distribution of household types with different vaccination statuses within the community. For

the remaining parameters, we create discrete distributions based on the information available for COVID-19 transmission characteristics, historical values for the effective reproduction number, and the advertised efficacy of approved vaccines.

- **Demographic data**: In our model is implemented with the actual population dataset from seven neighboring counties in Texas: Travis, Williamson, Bastrop, Caldwell, Hays, Burnet, and Blanco. The household type is a multivariate discrete distribution defined by: 1) the size of the household; 2) the vaccination status of the household; 3) the number of household members in different age groups. We consider the household size ranges from one to seven with different vaccination statuses and age group compositions.The distribution of household sizes and age group composition are downloaded from 5-year American Survey data (ACS) from `census.data.gov` for years 2014-2018 [76] and `https://usa.ipums.org/usa/` [77]. From sampled data, the IPUMS provides the weights of each household type with age group composition, and using the weights, the household types with age group composition are scaled up to represent the household type distribution. Out of seven counties, age group composition distribution is only available for Travis, Williamson, and Hays from IPUMS. Therefore, we assume that the age group composition is similar to that of Hays County for the remaining countries. As for the distribution of household vaccination status, there is no explicit database available. The distribution was estimated using the overall proportion of population vaccinated in Texas under different age groups [78]. The detailed demographic distribution data utilized in the experiments is provided in Supplementary File One.

- **Household transmission rate $b(\tilde{\omega})$:** Household transmission rate is a quantitative parameter that measures how contagious the disease is within a household in a community c. In some studies, this parameter is referred as household Secondary Attack Rate (SAR). The value of SAR, $b(\tilde{\omega})$ is between 0 and 1, and it represents the probability that an infection occurs among susceptible people within a household. In the extreme case, $b(\tilde{\omega}) = 0$ corresponds to no disease being transmitted within the household, and $b(\tilde{\omega}) = 1$ means all members within the household are infected [71]. In our model, we assume that members in the same household are highly likely to be infected by the same variant. Therefore, the distribution of household transmission rate depends on the virus variant. Currently, three notable COVID-19 variants are actively circulating in the U.S.: Alpha, Gamma, and

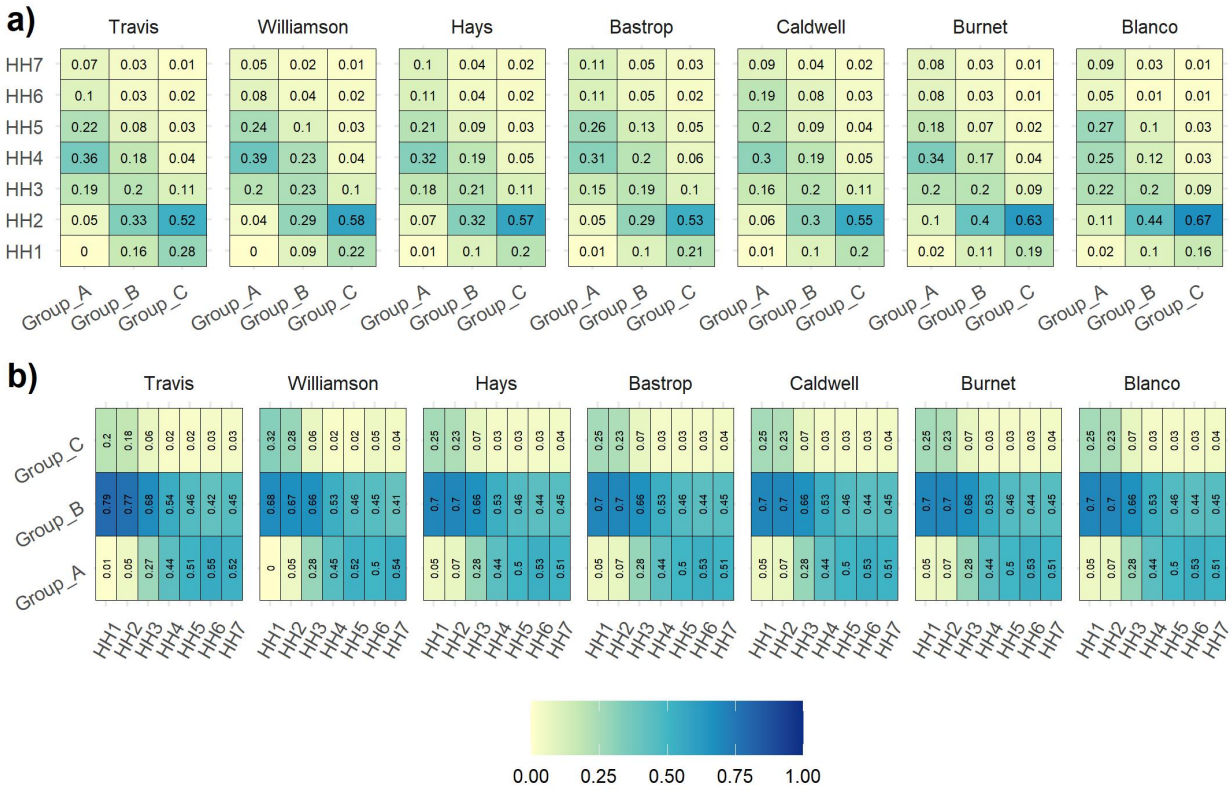

Figure 5.1: This figure shows the demographic distribution for each county. Figure a) shows the distribution of household sizes in each age group across all seven counties. Notice that the younger age group mostly resides in middle-size households, and Figure b) shows the distribution of age groups in each household size across seven counties.

Delta [79]. Tanaka et al. performed a cross-sectional study on SAR in households after the Alpha variant became dominant in Japan and estimated the Alpha SAR to be 38.7% [80]. Several studies have shown the potential increase in household transmission rate with Delta and Gamma variants compared to Alpha [81]. Regrading the current dominating Delta variant, it is estimated to be 1.66 times more transmissible than the Alpha variant. Based on the values in literature, we generated a discrete distribution for the within household transmission rate, $b(\tilde{\omega}_c)$.

- **Vaccine efficacy $\epsilon_k(\tilde{\omega}_c)$:** Mass vaccination efforts in the U.S. started at the beginning of 2021. A total of 370 million doses were administered, in which 54% were administered by August with Pfizer-BioNTech, 38% with Moderna, and the rest 8% with Johnson & Johnson [66]. According to several studies, vaccine efficacy $\epsilon(\tilde{\omega}_c)$ varies based on the COVID-19 variant. Pfizer-BioTech shows high

effectiveness, 88%-94% against Alpha variant [82, 83], with a reduction of 5 % towards Gamma and 10% towards Delta variants. For the Moderna vaccine, the efficacy is estimated to be around 90% against Alpha variant, and 89% against Delta variant [64]. The studies regarding the efficacy of the Johnson & Johnson vaccine towards different variants are very few. We will use the overall vaccine efficacy presented by Lopez et al. [83] to substitute for Johnson & Johnson. Based on these estimates, we generated vaccine efficacy distribution for households with vaccination status $i = 0$ in Supplementary File 1.

Probability	0.1			0.7			0.2		
$\epsilon(\tilde{\omega}_c)$	Pfizer	Moderna	Johnson	Pfizer	Moderna	Johnson	Pfizer	Moderna	Johnson
Alpha	0.97	0.95	0.67	0.94	0.92	0.64	0.88	0.86	0.58
Delta	0.90	0.88	0.63	0.87	0.85	0.60	0.81	0.80	0.53
Gamma	0.93	0.91	0.65	0.90	0.88	0.62	0.84	0.82	0.56
Other	0.94	0.92	0.65	0.91	0.89	0.62	0.85	0.83	0.56

Table 5.2: Vaccine efficacy $\epsilon(\tilde{\omega}_c)$ towards Alpha, Delta, Gamma and other variants

- **Relative susceptibility $\beta(\tilde{\omega}_c)$:** We consider age and vaccination status related differences in susceptibility to COVID-19. The *relative susceptibility* captures the variation in susceptibility due to the differences in social mixing and biological susceptibility between individuals. Current studies suggest that there is an increase in susceptibility with age for those who are not vaccinated yet [84, 85, 86]. Dattner et al. estimate that that the susceptibility of children (under 20 years old) is 43% (95% CI: [31%, 55%]) of the susceptibility of adults [87]. Due to the vaccine-induced immunity, the fully vaccinated people are less likely to be infected, in return, their susceptibility is relatively lower than those who are not vaccinated. Table 5.3 shows the relatively susceptibility of three age groups with different vaccination statuses.

- **Relative infectivity $\lambda(\tilde{\omega}_c)$:** The *relative infectivity* captures the variation in infectiousness between infected individuals due to the differences in social mixing and biological infectivity between individuals. For the population that is not vaccinated, reports show that younger age ($\leq$ 20 years) was associated with increased infectivity.Lau et al. statistically synthesize multiple data streams, and individuals under the age of 60 are 2.78 (95% CI:[2.10, 4.22]) times more infectious than the elderly

[88]. This nuance is essential to the transmission of COVID-19 because the younger population generally has more human interactions [89] and does not develop severe symptoms as compared to older populations. A member of the younger population, then, is more likely to infect a susceptible person. The relative infectivity for different age groups of a vaccinated population is not explicitly available. Several studies suggest that vaccines can reduce the symptoms but do not block the infection. Therefore, in this study, we assume that there is no difference in relative infectivity for the fully vaccinated group versus the not vaccinated group. The relative infectivity of three age groups with different vaccination statuses is presented in Table 5.3.

	Vaccination status = 0			Vaccination status =1		
Age group	Group A	Group B	Group C	Group A	Group B	Group C
Probability	0.03	0.41	0.08	0.24	0.23	0.02
Susceptibility	0.56	1.30	1.71	0.26	1.00	1.41
Infectivity	1.25	1.00	0.36	1.25	1.00	0.36

Table 5.3: Relative susceptibility and infectivity for Group A, Group B and Group C population with different vaccination statuses

- **Outside household close contact $m(\tilde{\omega}_c)$:** In our model, we treat the transmission in communities as a proliferation of infected households. Under this consideration, we need to know the average number of close contacts that an infective makes with persons of other households. Close contact means being sufficient for transmitting the disease when the contact is with a susceptible person. Here, $m(\tilde{\omega}_c)$ is a contact rate. Vaccination does not affect the number of contacts, but it affects the susceptibility and infectivity of individuals. Even though $m(\tilde{\omega}_c)$ is independent of vaccination, it varies due to differences in human interactions under the impact of various mitigation measures and demographics of a community. To estimate the distribution of $m(\tilde{\omega}_c)$ we used the following method:

  Note that in Equation 5.2, R_{HVc} is the effective reproduction number after vaccination. When the factors related to vaccination that are affecting the reproduction number can be excluded from the right hand, what is left is analogous to R_t. This can be achieved by setting $\epsilon(\omega_c) = 0$, and all $x_{nkvc} = 0$, for all $n \in \mathbb{N}, k \in \mathbb{K}, v \in 1, ..., p(n, v), c \in \mathbb{C}$. Basically Equation 5.2 is

reduced to $R_t = \sum_{n \in \mathbb{N}} a_{nk0c}(\tilde{\omega}_c) x_{nk0c}$. We can use R_t [90, 91] values and transmission rates for each variant to get m. The probability associated with m depends on the distribution of the variants and the proportion of time period the value of R_t was observed.

The discrete distribution for outside household contact $m(\tilde{\omega}_c)$ is available in Supplementary File 1.

- **Reliability level α for CC and ICC approach:** The acceptable reliability levels are typically prescribed by health officials based on the historical severity of the epidemic. With the parameters described in this section, we calculated the excess of effective reproduction number in each county under scenario ω when there are no vaccines in the future, denoted $e(\omega_c)$. Table 5.4 shows that the excess of effective reproduction number ranges from 0.6 to 4.7, which means that the effective reproduction number is [1.6, 5.7] across all scenarios. For this study, we use three reliability levels *High*, *Medium* and *Low* in ICC approach (see Table 5.5). Note that at the highest level of reliability, the acceptable expected excess is 0.5% of the expected excess $\mathbb{E}[e(\tilde{\omega}_c)]$ when there is no vaccines in the future, and for moderate and relaxed levels, the acceptable excess are set to 0.75% $\mathbb{E}[e(\tilde{\omega}_c)]$ and 1% $\mathbb{E}[e(\tilde{\omega}_c)]$, respectively. Table 5.6 presents the reliability levels γ used in CC approach.

County	Travis	Williamson	Bastrop	Caldwell	Hays	Burnet	Blanco
$\mathbb{E}[e(\tilde{\omega}_c)]$	2.590	2.532	2.361	2.257	2.416	1.961	1.715
Maximum violation	4.721	4.706	4.468	4.280	4.511	3.649	3.217
Minimum violation	0.994	0.926	0.829	0.788	0.876	0.712	0.611

Table 5.4: Expected, maximum and minimum excess for each county when no vaccines are allocated in the future.

Reliability level	Travis	Williamson	Bastrop	Caldwell	Hays	Burnet	Blanco
High	0.013	0.013	0.012	0.011	0.012	0.010	0.009
Medium	0.019	0.019	0.018	0.017	0.018	0.015	0.013
Low	0.026	0.025	0.024	0.023	0.024	0.020	0.017

Table 5.5: Reliability levels for each community used in ICC model

Reliability Level α	Travis	Williamson	Hays	Bastrop	Caldwell	Burnet	Blanco
High	0.04	0.04	0.04	0.04	0.04	0.04	0.04
Medium	0.08	0.08	0.08	0.08	0.08	0.08	0.08
Low	0.12	0.12	0.12	0.12	0.12	0.12	0.12

Table 5.6: Reliability levels for each community used in CC model.

5.5 Results and Discussion

In this section, we present the results of the stochastic model under different reliability levels. The stochastic model was solved using a set of predetermined levels of α_c and γ_c along with the discrete distributions given in Section 5.4 for the uncertain parameters such as transmission rate, vaccine efficacy, close contact rate, relative susceptibility, and relative infectivity under different vaccination statuses. In general, for more populated communities, individuals that have more frequent social interactions can lead to a greater likelihood of an outbreak of a contagious disease. The outbreak eventually can spread to the surrounding communities if the more populated community is not under control. Therefore, health officials should prepare for outbreaks in population centers and their surrounding communities. In this study, we consider seven counties in Texas, Travis, Williamson, Bastrop, Caldwell, Hays, Burnet, and Blanco, in which Travis is the center of the outbreak with the largest population. We perform several case studies to generate vaccination policies for all seven counties under all these uncertain parameters by driving the post-vaccination reproduction number $R_{HV_c} \leq 1$.

For each level of reliability, we solve instances of the model for all counties. The vaccination policy suggested by ICC and CC model is not only governed by uncertain parameters, but also by the population demographics in each county. The population demographics include the distribution of the household sizes, age compositions in a household, and vaccination status of the household members. The vaccination policy prescribes the minimum proportion of a population with different vaccination statuses required to be vaccinated to control the outbreak in each county.

We report the proportion of population to vaccinate in each county under High, Medium, and Low reliability levels for both ICC and CC approach in Figure 5.2 and 5.3 respectively. The results show similar trends for all three levels in each county. From ICC model under High reliability level, the proportions of the total population required to be vaccinated to control the epidemic for Travis, Williamson, Hays, Bastrop,

Calwell, Burnet, and Blanco are 0.66, 0.65, 0.60, 0.60, 0.64, 0.60, and 0.52, respectively. From CC model under High reliability level, the proportions of the total population required to be vaccinated to control the epidemic for Travis, Williamson, Hays, Bastrop, Calwell, Burnet, and Blanco are 0.65, 0.64, 0.63, 0.62, 0.62, 0.59, and 0.56, respectively. As described in Section 2.1.2, reformulation of CC approach is a mixed-integer programming. In general, the computation cost is high. Table 5.7 shows that after six hours, CC instances still have a relatively large gap, where gap is defined as the absolute difference between the best bound and the best integer solution divided by best integer solution. In contrast, ICC instances are solved in less than four minutes. CC approach provides a similar vaccination policy to ICC approach across all three reliability levels. Therefore, in the rest of this section, we present only ICC results.

	ICC			CC		
Reliability level	High	Medium	Low	High	Medium	Low
Gap	2.59%	2.62%	5.9%	0%	0%	0%
Time (seconds)	15000	15000	15000	154	167	203

Table 5.7: Computation time (seconds) and solution gap for CC and ICC model under High, Medium and Low reliability level

We observe that for a more populated county, we need to vaccinate a higher proportion of the population to control the epidemics. When looking at the percentage of a population to vaccinate regarding vaccination status, both models prefer to vaccinate more people that have not been vaccinated yet. This is probably because those who are not vaccinated are more susceptible than those who are already vaccinated. This is true for all three reliability levels. In Travis county, under High reliability level, we suggest to vaccinate 66% of the total population, which is 87% of the population that has vaccination status $k = 0$, and 46% of the population has vaccination status $k = 1$ as shown in Figure 5.4. For counties with smaller populations, there is a noticeable reduction in the proportion of the population to vaccinate for vaccination status $k = 0$. In contrast, for vaccination status $k = 1$, the proportion to vaccinate stays almost at the same level regardless of population sizes. This is because they were already vaccinated and had a good immunity. They are not as risk as vaccination $k = 0$ group to spread the disease. From the figure, we also observe that when we lower the reliability levels, there is a significant drop in the proportion of population not vaccinated. For those who

have already been vaccinated, proportions stay almost at the same level across all reliability levels.

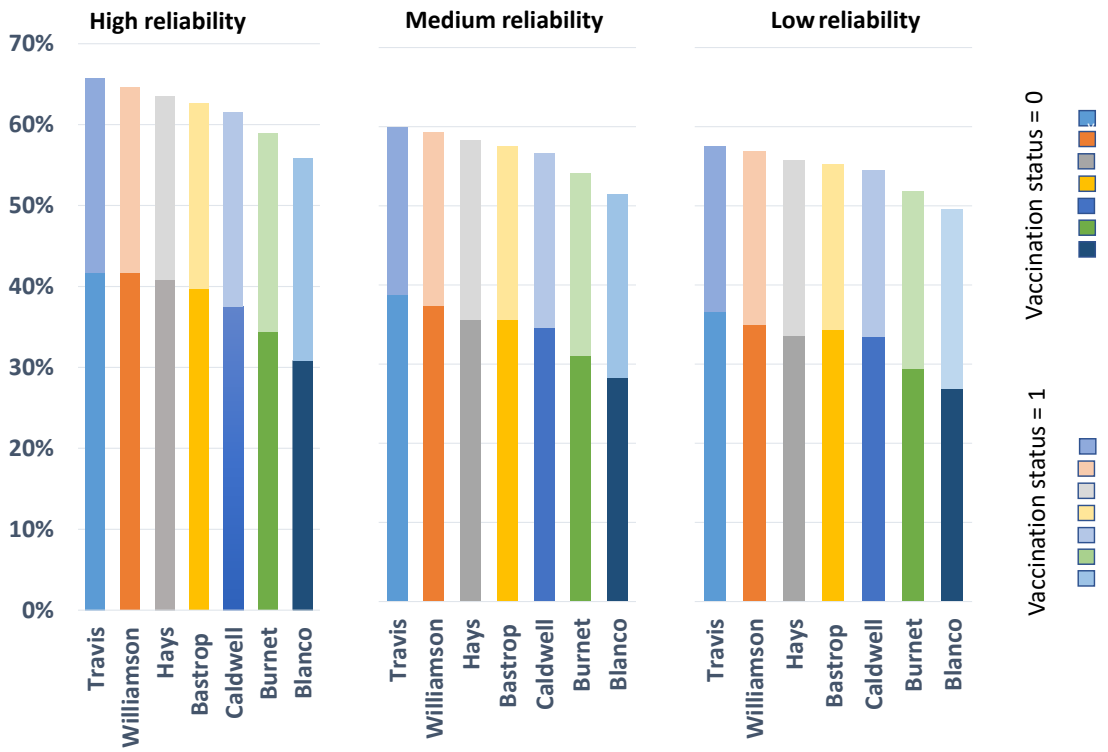

Figure 5.2: Proportion of total population to vaccinate in each county under High, Medium, and Low reliability levels from ICC model

Households are an important contributor and high risk setting for COVID-19 transmission [92] and are a critical factor in wider community spread [93]. The recent variants have a relatively high transmission rate within a household. If a member in a household is infected, the other members who live in the same household are more likely to be infected. For those who reside in larger household sizes, if one of them is infected, there are more members to spread the disease to than those who reside in smaller households. The results indicate that counties should vaccinate a relatively higher proportion of larger size non-vaccinated households and not vaccinate any household of size one as shown in Figure 5.5. For households that have been vaccinated, the proportion of population to vaccinate in different sizes of households varies based on the vaccination status and other population demographic features in each county with no obvious trend. The observations are similar across all reliability levels. For detailed results on the proportion of the population to

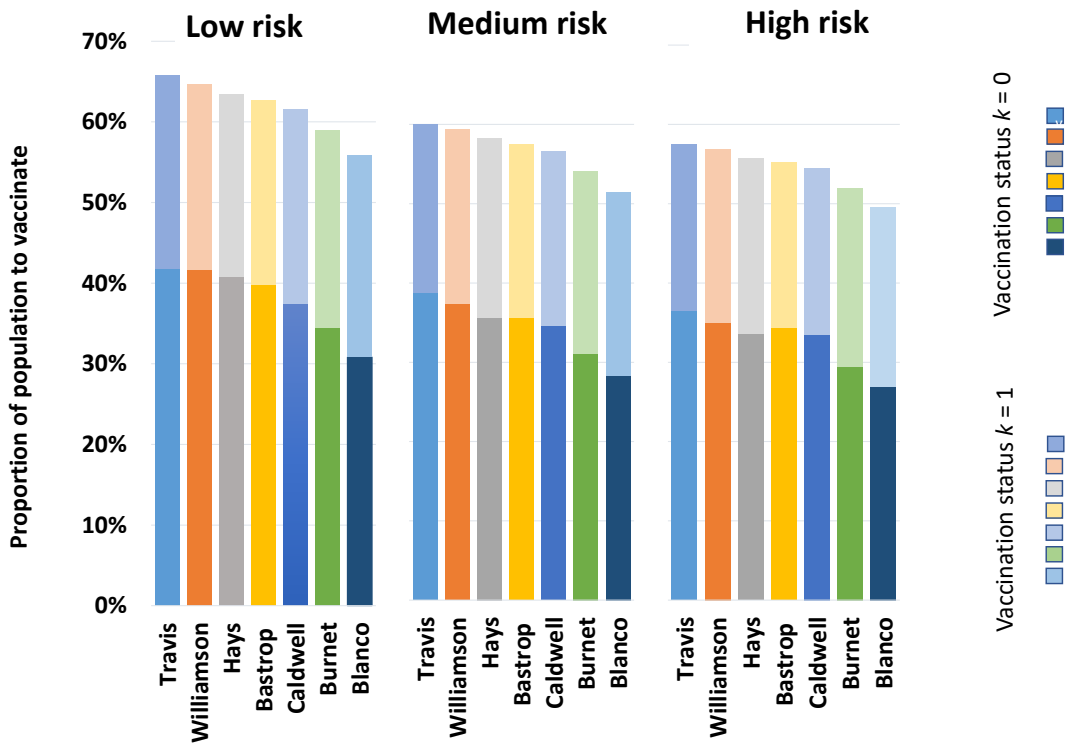

Figure 5.3: Proportion of total population to vaccinate in each county under High, Medium, and Low reliability levels from CC model

	High reliability		Medium reliability		Low reliability	
County	Vaccination status k=0	Vaccination status k=1	Vaccination status k=0	Vaccination status k=1	Vaccination status k=0	Vaccination status k=1
Travis	86.44%	46.44%	80.25%	41.07%	75.65%	40.55%
Williamson	83.68%	45.80%	75.10%	43.76%	70.16%	43.67%
Hays	82.03%	45.02%	71.54%	45.05%	67.72%	43.96%
Bastrop	78.11%	46.67%	70.04%	44.62%	67.55%	42.53%
Caldwell	74.20%	48.74%	68.56%	44.57%	66.12%	42.56%
Burnet	72.64%	46.62%	65.59%	43.68%	62.08%	42.68%
Blanco	66.02%	46.92%	60.57%	43.45%	57.60%	42.49%

Table 5.8: Proportion of population with different vaccination statuses to vaccinate in each county under high, medium and low reliability level

vaccinate with each vaccination status per household type across all reliability levels, refer to Supplementary File 2.

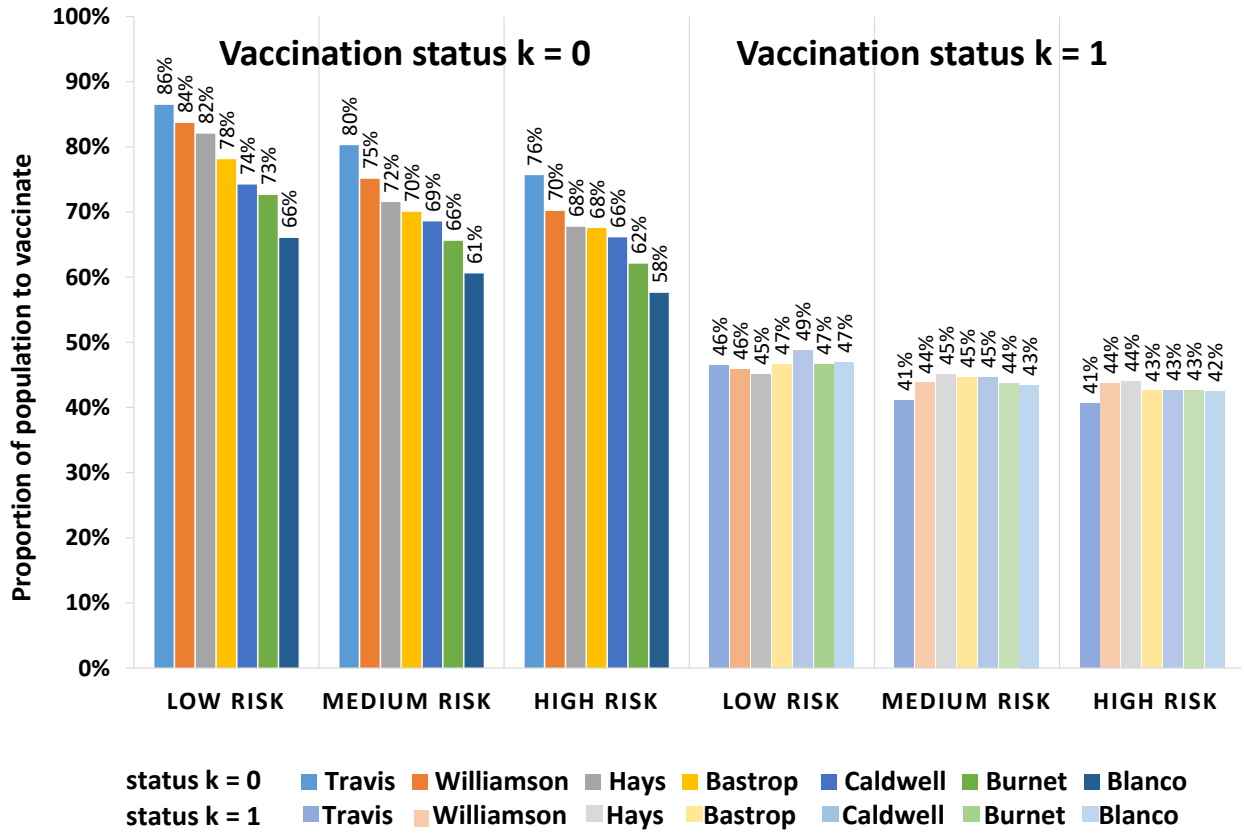

Figure 5.4: Proportion of population with different vaccination statuses to vaccinate under High, Medium and Low reliability levels for ICC model

Understanding the role of age in transmission and symptom severity is critical for determining the vaccination policy. Without effective control measures, regions with larger populations that have relatively high susceptibility can spread the disease much faster. Under this rationale, in the U.S., at the early stage of vaccination deployment, the elderly are the very first tier to get vaccinated in the general population. Figure 5.6 illustrates the proportion of populations with different vaccination statuses to vaccinate in each age group under three reliability levels. It suggests to release more vaccines to Group B, followed by Group A and Group C. There are two major reasons why Group C is allocated proportionally fewer vaccines. Firstly, at the time of writing this study, 80% of the older population, age ≥ 65, are already vaccinated. They gained some immunity from the vaccines and are not as susceptible as the not vaccinated group. Secondly, the population in Group C primarily reside in smaller households, household size of one or two. If they are infected, there are few members to spread the disease to within the household. In contrast, the Group A and Group

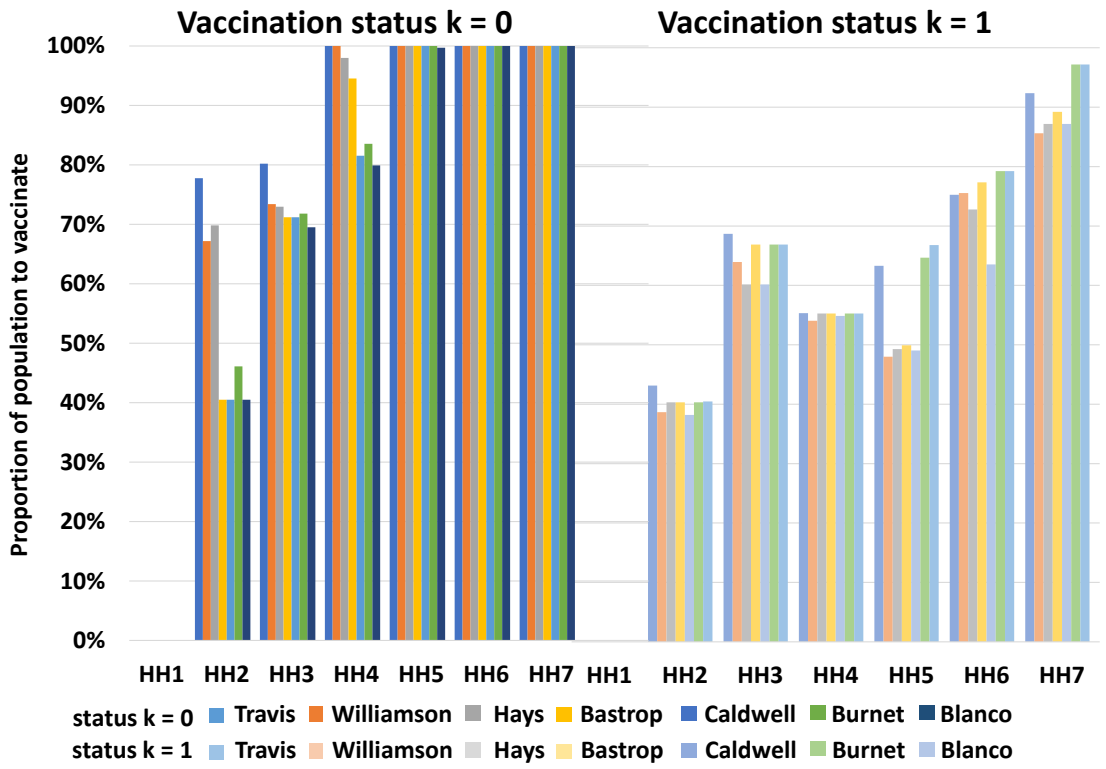

Figure 5.5: Proportion of population with different vaccination statuses to vaccinate in each household size (HH) for each county under High reliability level (this trend holds for Medium and Low reliability levels

B populations live in relatively larger household sizes compared to the Group C population. If Group B or Group C people are infected, within the household that they live in, there are more members to transmit the disease to. In addition, Group A and Group B populations are more likely to live in the same household of size three and up. We know that Group B population is relatively more susceptible to the disease compared to Group A population. For a member in the household, Group B population has a higher chance to be infected, compared to the other Group A population in the same household. Therefore, to effectively control the outbreak, our model suggests to vaccinate a larger proportion of Group B to prevent them from getting the disease and spreading the disease to others.

5.6 Conclusion

We consider an integrated chance-constraint and chance-constrained methodology for incorporating uncertain parameters for finding optimal vaccination policies for epidemics. We specifically derived the ap-

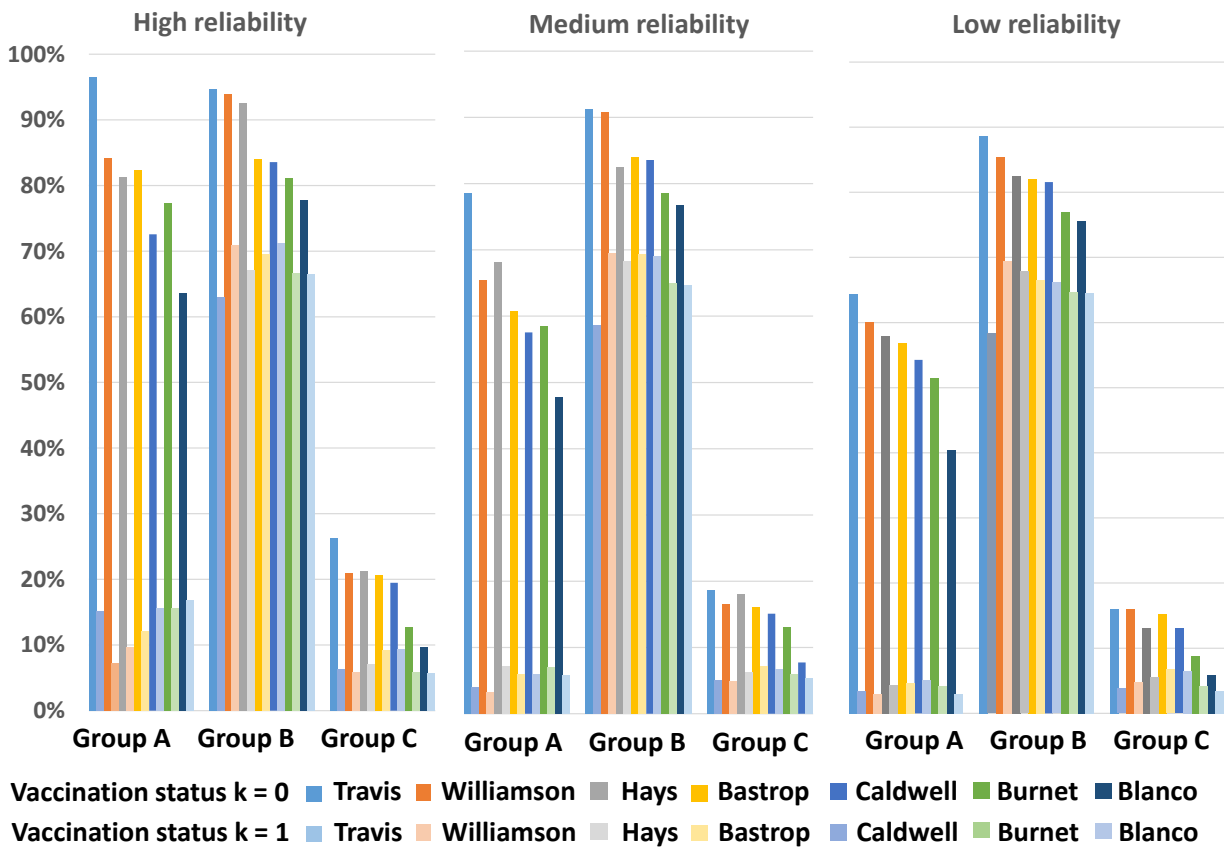

Figure 5.6: Proportion of three age group populations with different vaccination statuses to vaccinate under High, Medium and Low reliability levels

proach determines household-based vaccination policies to control the outbreak of COVID-19 under three predetermined reliability levels. A policy captures the demographic structure of households, age-related heterogeneity in susceptibility and infectivity, and population vaccination status. The model was implemented for seven neighboring counties in the U.S. state of Texas, one of which is the center of the outbreak with largest population size. Under high reliability level, the results suggest to vaccinate 75% of the population that are not vaccinated and give a booster shot to 43% of the population who have already been vaccinated. Understanding the role of age in transmission and symptom severity is critical for determining the vaccination policy. Without effective control measures, regions with a larger population that have relatively high susceptibility can spread the disease disproportionally faster. Therefore, the model suggests to release proportionally more vaccines to Group B, followed by Group A and Group C. The results also real that a more effective vaccination policy for controlling an outbreak is to vaccinate households with larger sizes. The

reason as that a larger size household, if a member is infected, there are more members to spread the disease compared to a smaller household. Future work along this line of research includes considering vaccines logistic while deciding vaccination policies, such as vaccination transportation, storing, and distribution.

6. SUMMARY AND FUTURE WORK

This dissertation explores three stochastic programming models and solutions for two different health care related applications involving uncertain parameters, namely; pathways scheduling for connected community health, and optimal vaccination policies for Covid-19. The three approaches of stochastic programming are investigated in this dissertation are: 1) stochastic programming with recourse in which infeasibility is not allowed, only recourse/corrective actions with a certain cost; 2) chance-constrained programming in which infeasibility is allowed; and 3) integrated chance-constrained programming where infeasibility is accepted, but the violation amount is bounded. When decisions are made at different stages and allow corrective actions in the future stage, stochastic programming with recourse approach can be applied. For applications where infeasibility is allowed under some scenarios, CC and ICC are appropriate approaches. However, if the violation amount is critical to the application, ICC should be applied. The first approach is applied to a community health pathways scheduling problem from healthcare, while the last two methodologies are applied to optimal vaccine allocation under uncertainty, with a focus for COVID-19.

6.1 Summary

Scheduling and coordinating constrained resources in community healthcare settings at a centralized community level is challenging due to limited resources and the inherent dynamics of the processes and the organizational structures. Community health pathways (CHPs) have been introduced as a standardized interdisciplinary tool that details multiple steps of a healthcare-related service and the required resources for each step. However, the time window constraints for each step and the data uncertainty in resource availability make this scheduling problem very challenging. On the other hand, rising demand and costs of healthcare motivate the need for efficient schedules. In this work, we developed a stochastic programming model to schedule CHPs and community healthcare resources under resource availability uncertainty.

A computational study based on a real Pathways Community HUB setting provided several findings and managerial insights. The results show that the schedules provided by the deterministic model can be too optimistic and may not necessarily work well under uncertainty in resource availability. client wait time depends on client demand, with high demand resulting in longer waiting time. The study also shows that workload balancing is preferred because it provides schedules with similar workloads across resources

of the same type, while providing waiting times that are comparable to when no workload balancing is applied. Managerial insights include the recommendation to HUB managers and schedulers to use workload balancing not only to minimize client waiting time, but also to guarantee client schedules that result in equitable use of limited resources in the Pathways Community HUB.

For the optimal vaccination allocation problem, we develop an integrated chance-constraint model that includes uncertain parameters for finding optimal vaccination policies. We derived household-based vaccination policies to control the outbreak of COVID-19 under three predetermined reliability levels. Our policy captures the demographic structure of households, age-related heterogeneity in susceptibility and infectivity, and population vaccination status. The model was implemented in seven neighboring counties in the U.S. state of Texas, one of which is the center of the outbreak with a larger population size. Under high reliability level, the results suggest to vaccinate 75% of the population that are not vaccinated and give a booster shot to 43% of the population who have already been vaccinated. Understanding the role of age in transmission and symptom severity is critical for determining the vaccination policy. Without effective control measures, regions with a larger population that have relatively high susceptibility can spread the disease much faster. The solution also suggests to release more vaccines to Group B, followed by Group A and Group C. The solution also indicates that a more effective vaccination policy for controlling an outbreak is to vaccinate households with larger sizes. The reason as that in a larger size household, if a member is infected, there are more members to spread the disease to compared in a smaller household.

6.2 Limitations and Future Research

The CHPs scheduling methodology developed in this dissertation is a step forward towards addressing pathway scheduling problems. However, there are a few remaining aspects to the problem which serve as motivation for future research. Problem uncertainty is reflected in resource availability. One extension is to consider client no-shows for scheduled appointments. For pathways, if a client does not show up for the appointment of a particular step, they can either end the pathway or reschedule. As future work, no-shows can be incorporated in the methods by assuming a certain percentage of the pathway steps are rescheduled or modified. Whenever there is a no-show, the model needs to release those resources that are assigned to future steps of that pathway. If a client prefers to continue the pathway, then the model must make a new request to schedule the rest of the pathway based on the future availability of the resources involved.

Incorporating this rescheduling feature will more accurately capture the real Pathways Community HUB setting.

In the optimization model, the current formulation determines the pathway starting date and does not offer clients to choose their preferable start dates. Another extension to this work is to reformulate the problem to incorporate client preference in the starting date and time. In this work, the SP model is solved directly via the DEP using a direct solver. Hence, the computational cost is relatively high. Therefore, there is a need to develop a decomposition algorithm to speed up computation time for the scheduling problem. For Pathways Community HUBs dealing with CHPs involving high-risk clients, one can also devise a risk-averse stochastic programming model to take risk into consideration.

COVID-19 is still soaring with new SARS-Cov2 virus mutations. Without a cure, we need new vaccines to help control the disease. The vaccination strategy suggested by our model is household-based, and the vaccination status is labeled based-on the household as a unit. If a household has vaccination status equal to one, then we assume that all members in that household are vaccinated. However, a large proportion of the population which is 20 years old and younger was not yet vaccinated at the time of this study. To model reality more accurately, we need to adjust the assumption on vaccination status in our future work. One possible option is to label vaccination status with respect to the age group in a household. In this way, younger age population vaccination status can be represented more accurately.

The CC and ICC models introduced in this work capture uncertainty in transmission characteristics and variability in population demographics, and determines who should be vaccinated under different reliability levels. However, logistics for vaccine storage, handling, and management are not covered in this dissertation. Failure to store and handle vaccines properly can result in inadequate immune responses in individuals and poor protection against COVID-19. As future work, the logistics aspects of vaccine transportation and storage will need to be considered.

7. First Appendix

7.1 Supplementary File 1:

This file includes all model parameters presented in Chapter 5 and scenarios for each county.

7.2 Supplementary File 2:

This file includes detailed solution for Chapter 5.

REFERENCES

[1] E. Gee and T. Spiro, "Excess administrative costs burden the U.S. health care system," tech. rep., Center for American Progress, 2019. https://cdn.americanprogress.org/content/uploads/2019/04/03105330/Admin-Costs-brief.pdf.

[2] R. Burton, "Improving care transitions, health policy brief," tech. rep., Health Affairs, 2012. DOI: 10.1377/hpb20120913.327236.

[3] R. Mclellan, B. Sherman, R. Loeppke, J. Green Mckenzie, K. Mueller, C. Yarborough, P. Grundy, H. Allen, and P. W Larson, "Optimizing health care delivery by integrating workplaces, homes, and communities how occupational and environmental medicine can serve as a vital connecting link between accountable care organizations and the patient-centered medical home," *Journal of occupational and environmental medicine / American College of Occupational and Environmental Medicine*, vol. 54, pp. 504–12, 2012.

[4] B. P. Zeigler, S. A. Redding, B. A. Leath, and E. L. Carter, "Pathways community hub: A model for coordination of community health care," *Population Health Management*, vol. 17, pp. 199–201, 2014.

[5] J. Bernal, N. Andrews, C. Gower, E. Gallagher, R. Simmons, S. Thelwall, E. Tessier, N. Groves, G. Dabrera, R. Myers, C. Campbell, G. Amirthalingam, M. Edmunds, M. Zambon, K. Brown, S. Hopkins, M. Chand, and M. Ramsay, "Effectiveness of covid-19 vaccines against the b.1.617.2 variant," *The New England Journal of Medicine*, vol. 385, pp. 585–594, 05 2021.

[6] B. Sheikh, J. McMenamin, B. Taylor, C. Robertson, P. H. Scotland, and the EAVE II Collaborators, "Sars-cov-2 delta voc in scotland: demographics, risk of hospital admission, and vaccine effectiveness," *Lacent*, vol. 397, pp. 2461–2462, 06 2021.

[7] R. Hughes, ed., *Patient Safety and Quality: An Evidence-Based Handbook for Nurses*. Rockville, MD, USA: National Academies Press (US), apr. pmid: 2132875 ed., 2008.

[8] A. Shapiro, D. Dentcheva, and A. Ruszczyński, *Lectures on stochastic programming. Modeling and theory*. Society for Industrial and Applied Mathematics, 01 2009.

[9] C. S. ReVelle, W. R. Lynn, and F. Feldmann, " Mathematical Models for the Economic Allocation of Tuberculosis Control Activities in Developing Nations," *Am. Rev. Respir. Dis.*, vol. 96, no. 5, pp. 893–909, 1967.

[10] W. K. Klein Haneveld, "On integrated chance constraints," in *Stochastic Programming* (F. Archetti, G. Di Pillo, and M. Lucertini, eds.), (Berlin, Heidelberg), pp. 194–209, Springer Berlin Heidelberg, 1986.

[11] W. Haneveld and M. Vlerk, "Integrated Chance Constraints: Reduced Forms and an Algorithm," *Computational Management Science*, vol. 3, no. 4, pp. 245–269, 2006.

[12] R. J. Garstka, S. J.and Wets, "On decision rules in stochastic programming," *Mathematical Programming*, vol. 7, pp. 117–143, 1974.

[13] G. B. Dantzig, "Linear programming under uncertainty," *Management Science*, vol. 1, no. 3/4, pp. 197–206, 1955.

[14] G. B. Dantzig and P. Wolfe, "Decomposition Principle for Linear Programs," *Operations Research*, vol. 8, no. 1, pp. 101–111, 1960.

[15] G. B. Dantzig and P. Wolfe, "The Decomposition Algorithm for Linear Programs," *Econometrica*, vol. 29, no. 4, pp. 101–111, 1961.

[16] J. F. Benders, "Partitioning procedures for solving mixed-variables programming problems," *Numerische Mathematik*, vol. 4, pp. 238–252, 1962.

[17] F. Louveaux and J. R. Birge, *L-shaped method for two-stage stochastic programs with recourse*, pp. 1208–1210. Boston, MA: Springer, 2001.

[18] R. M. V. Slyke and R. Wets, "L-Shaped Linear Programs with Applications to Optimal Control and Stochastic Programming," *Journal on Applied Mathematics*, vol. 17, no. 4, pp. 638–663, 1969.

[19] J. L. Higle and S. Sen, "Stochastic Decomposition: An Algorithm for Two-Stage Linear Programs with Recourse," *Mathematics of Operations Research*, vol. 16, no. 3, pp. 650–669, 1991.

[20] S. Sen, "Subgradient decomposition and differentiability of the recourse function of a two stage stochastic linear program," *Operations Research Letters*, vol. 13, no. 3, pp. 143–148, 1993.

[21] L. Ntaimo, "Disjunctive Decomposition for Two-Stage Stochastic Mixed-Binary Programs with Random Recourse," *Operations Research*, vol. 58, no. 1, pp. 229–243, 2010.

[22] A. J. Kleywegt, A. Shapiro, and T. H. de Mello, "The Sample Average Approximation Method for Stochastic Discrete Optimization," *Journal on Optimization*, vol. 12, no. 2, pp. 479–502, 1969.

[23] A. Charnes and W. W. Cooper, "Chance-Constrained Programming," *Management Science*, vol. 6, no. 1, pp. 73–79, 1959.

[24] A. Charnes and W. W. Cooper, "Deterministic Equivalents for Optimizing and Satisficing under Chance Constraints," *Operations Research*, vol. 11, no. 1, pp. 18–39, 1963.

[25] K. Shinji, "A Stochastic Programming Model," *Econometrica*, vol. 31, no. 1/2, pp. 181–196, 1963.

[26] A. Prékopa, "Contributions to the theory of stochastic programming," *Mathematical Programming*, vol. 4, pp. 202–221, 1973.

[27] D. Dentcheva, A. Prékopa, and A. Ruszczynski, "Concavity and efficient points of discrete distributions in probabilistic programming," *Mathematical Programming*, vol. 89, no. 1, pp. 55–77, 1963.

[28] S. Sen, " Relaxations for probabilistically constrained programs with discrete random variables ," *Operations Research Letters*, vol. 11, no. 2, pp. 81–86, 1992.

[29] P. Beraldi and M. E. Bruni, "An exact approach for solving integer problems under probabilistic constraints with random technology matrix," *Annals of Operations Research*, vol. 177, pp. 127–137, 2010.

[30] J. Luedtke, "A branch-and-cut decomposition algorithm for solving chance-constrained mathematical programs with finite support," *Mathematical Programming volume*, vol. 1, pp. 219–244, 2014.

[31] W. K. K. Haneveld, M. H. Streutker, and M. H. van der Vlerk, " An ALM model for pension funds using integrated chance constraints ," *Annals of Operations Research*, vol. 177, pp. 47–62, 2010.

[32] M. K. M., Schultz, L. Albin, N. Pineda, J. Lonhart, V. Sundaram, C. Smith-Spangler, J. Brustrom, E. Malcolm, L. Rohn, and S. Davies, "Chapter 2. what is care coordination?," *Agency for Healthcare Research and Quality*, 2014. https://www.ahrq.gov/ncepcr/care/coordination/atlas/chapter2.html.

[33] H. K. Koh, G. Graham, and S. A. Glied, "Reducing racial and ethnic disparities: The action plan from the department of health and human services," *Health Affairs*, vol. 30, no. 10, 2011. DOI: 10.1377/hlthaff.2011.0673.

[34] Agency for Healthcare Research and Quality, "Coordination care for adults with complex care needs in the patient centered medical home: Challenges and solutions," 2012. White Paper.

[35] Community Care Coordination Learning Network, "Connecting those at risk to care: The quick start guide to developing community care coordination pathways," 2011. Agency for Healthcare Research and Quality, https://www.ahrq.gov/innovations/hub/quickstart-guide.html.

[36] T. Rotter, L. Kinsman, E. James, A. Machotta, H. Gothe, J. Willis, P. Snow, and J. Kugler, "Clinical pathways: effects on professional practice, patient outcomes, length of stay and hospital costs," *Cochrane Database of Systematic Reviews*, no. 3, 2010.

[37] C. L. Damberg, M. E. Sorbero, S. L. Lovejoy, G. Martsolf, L. Raaen, and D. Mandel, "Measuring success in health care value-based purchasing programs summary and recommendations," 03 2014.

[38] G. Du, Z. Jiang, Y. Yao, and X. Diao, "Clinical pathways scheduling using hybrid genetic algorithm," *Journal of Medical Systems*, vol. 37, pp. 1–17, 2013.

[39] A. Wolf, "Constraint-based modeling and scheduling of clinical pathways," in *Recent Advances in Constraints* (J. Larrosa and B. O'Sullivan, eds.), Lecture Notes in Artificial Intelligence, pp. 122–138, Berlin, Germany: Springer-Verlag, 2009.

[40] A. Scherer and A. McLean, "Mathematical models of vaccination," *British Medical Bulletin*, vol. 62, pp. 187–199, 07 2002.

[41] M. W. Tanner, L. Sattenspiel, and L. Ntaimo, "Finding optimal vaccination strategies under parameter uncertainty using stochastic programming," *Mathematical Biosciences*, vol. 215, pp. 144–151, 2008.

[42] N. L. Bragazzi, V. Gianfredi, M. Villarini, R. Rosselli, A. Nasr, A. Hussein, M. Martini, and M. Behzadifar, "Vaccines meet big data: State-of-the-art and future prospects. from the classical 3is ("isolate–inactivate–inject") vaccinology 1.0 to vaccinology 3.0, vaccinomics, and beyond: A historical overview," *Frontiers in Public Health*, vol. 6, 2018. doi: 10.3389/fpubh.2018.00062.

[43] H. Waaler, A. Geser, and S. Andersen, "The Use of Mathematical Models in the Study of the Epidemiology of Tuberculosis," *Am. J. Public Health*, vol. 52, no. 6, pp. 1002–1013, 1962.

[44] H. W.Hethcote and P. Waltman, " Optimal vaccination schedules in a deterministic epidemic model," *Math. Biosci*, vol. 18, no. 3-4, pp. 365–381, 1973.

[45] F. Ball, D. Mollison, and G. Scalia-Tomba, " Epidemics with two levels of mixing ," *Ann. Appl. Probab.*, vol. 7, no. 1, pp. 46–89, 1997.

[46] H. Yarmand, J. Ivy, B. Denton, and A. Lloyd, "Optimal two-phase vaccine allocation to geographically different regions under uncertainty," *European Journal of Operational Research*, vol. 233, pp. 208–219, 2014.

[47] S.-I. Chen and C.-Y. Wu, "A stochastic programming model of vaccine preparation and administration for seasonal influenza interventions," *Mathematical Biosciences and Engineering*, vol. 17, pp. 2984–2997, 2020.

[48] N. G.Becker and D. N.Starczak, "Optimal vaccination strategies for a community of households.," *Math. Biosci*, vol. 139 2, pp. 117–32, 1997.

[49] M. W. Tannera, L. Sattenspiel, and L. Ntaimo, " Finding optimal vaccination strategies under parameter uncertainty using stochastic programming ," *Math. Biosci*, vol. 215, no. 1-2, pp. 144–151, 2008.

[50] T. Rotter, R. B. de Jong, S. E. Lacko, U. Ronellenfitsch, and L. Kinsman, "Clinical pathways as a quality strategy," in *Improving healthcare quality in Europe: Characteristics, effectiveness and implementation of different strategies*, UN City, Copenhagen, Denmark: WHO Regional Office for Europe, 2019.

[51] D. Mechanic and J. Tanner, "Vulnerable people, groups, and populations: Societal view," *Health Affairs*, vol. 26, no. 5, pp. 1220–1230, 2007. PMID: 17848429.

[52] Bandolier Forum, "Independent evidence-based health care: On care pathways," 2003.

[53] C. N. Gross, J. O. Brunner, and M. Blobner, "Hospital physicians can't get no long-term satisfaction – an indicator for fairness in preference fulfillment on duty schedules," *Health Care Management Science*, vol. 22, pp. 691–708, 2019.

[54] M. Issabakhsh, S. Lee, and H. Kang, "Scheduling patient appointment in an infusion center: a mixed integer robust optimization approach," *Health Care Management Science*, 2020. doi:https://doi.org/10.1007/s10729-020-09519-z.

[55] B. Vieira, D. Demirtas, J. B. van de Kamer, E. W. Hans, L.-M. Rousseau, N. Lahrichi, and W. H. van Harten, "Radiotherapy treatment scheduling considering time window preferences," *Health Care Management Science*, vol. 23, pp. 520–534, 2020.

[56] S. Srinivas and A. R. Ravindran, "Designing schedule configuration of a hybrid appointment system for a two-stage outpatient clinic with multiple servers," *Health Care Management Science*, vol. 23, pp. 360–386, 2020. https://doi.org/10.1007/s10729-019-09501-4.

[57] J. R. Munavalli, S. V. Rao, A. Srinivasan, and G. van Merode, "Integral patient scheduling in outpatient clinics under demand uncertainty to minimize patient waiting times," *Health Informatics Journal*, vol. 26, no. 1, pp. 435–448, 2019.

[58] CPLEX, *IBM ILOG CPLEX Optimization Studio CPLEX User's Manual*. Armonk, NY: IBM Corporation, 2019.

[59] J. A. P. Heesterbeek and K. Dietz, "The concept of Ro in epidemic theory," *Statistica Neerlandica*, vol. 50, no. 1, pp. 89–110, 1996.

[60] P. Delamater, E. Street, T. Leslie, Y. Yang, and K. Jacobsen, "Complexity of the basic reproduction number (R0)," *Emerging Infectious Diseases*, vol. 25, pp. 1–4, 01 2019.

[61] H. Nishiura and G. Chowell, "The Effective Reproduction Number as a Prelude to Statistical Estimation of Time-Dependent Epidemic Trends," *Mathematical and Statistical Estimation Approaches in Epidemiology*, pp. 103–121, 2009.

[62] T.-C. Ng and T.-H. Wen, "Spatially adjusted time-varying reproductive numbers: Understanding the geographical expansion of urban dengue Outbreaks," *Scientific Reports*, vol. 9, 2019. doi:10.1038/s41598-019-55574-0.

[63] "Different covid-19 vaccines." Web, November 2011.

[64] L. Baden, H. Sahly, B. Essink, K. Kotloff, S. Frey, R. Novak, D. Diemert, S. Spector, N. Rouphael, C. Creech, J. McGettigan, S. Kehtan, N. Segall, J. Solis, A. Brosz, C. Fierro, H. Schwartz, K. Neuzil, L. Corey, and T. Zaks, "Efficacy and safety of the mrna-1273 sars-cov-2 vaccine," *New England Journal of Medicine*, vol. 384, pp. 403–416, 12 2020.

[65] C. Pawlowski, P. Lenehan, A. Puranik, V. Agarwal, A. Venkatakrishnan, M. J. Niesen, J. C. O'Horo, A. Virk, M. D. Swift, A. D. Badley, J. Halamka, and V. Soundararajan, "Fda-authorized mrna covid-19 vaccines are effective per real-world evidence synthesized across a multi-state health system," *Med*, vol. 2, no. 8, pp. 979–992.e8, 2021.

[66] Centers for Disease Control and Prevention, "Covid data tracker, variant proportions." Web.

[67] K. M. Bubar, K. Reinholt, S. M. Kissler, M. Lipsitch, S. Cobey, Y. H. Grad, and D. B. Larremore, "Model-informed covid-19 vaccine prioritization strategies by age and serostatus," *Science*, vol. 371, no. 6532, pp. 916–921, 2021.

[68] M. A. Acuña-Zegarra, S. Díaz-Infante, D. Baca-Carrasco, and D. Olmos-Liceaga, "Covid-19 optimal vaccination policies: A modeling study on efficacy, natural and vaccine-induced immunity responses," *Mathematical Biosciences*, vol. 337, 2021. doi:https://doi.org/10.1016/j.mbs.2021.108614.

[69] L. Matrajt, J. Eaton, T. Leung, and E. R. Brown, "Vaccine optimization for covid-19: Who to vaccinate first?," *Science Advances*, vol. 7, no. 6, 2020. doi:10.1126/sciadv.abf1374.

[70] R. M. Anderson, H. Heesterbeek, D. Klinkenberg, and T. D. Hollingsworth, "How will country-based mitigation measures influence the course of the COVID-19 epidemic?," *The Lancet*, vol. 395, no. 10228, pp. 931–934, 2020.

[71] N. G. Becker and D. N. Starczak, "Optimal vaccination strategies for a community of households," *Mathematical Biosciences*, vol. 139, pp. 117–132, Jan. 1997.

[72] Centers for Disease Control and Prevention, "Covid data tracker, demographic characteristics of people receiving covid-19 vaccinations in the united states." `https://www.cdc.gov/coronavirus/2019-ncov/vaccines/distributing/demographics-vaccination-data.html`.

[73] Y. Wang, Y. Liu, J. Struthers, and M. Lian, "Spatiotemporal characteristics of the covid-19 epidemic in the united states," *Clinical Infectious Diseases*, 2020. doi: 10.1093/cid/ciaa934.

[74] Centers for Disease Control and Prevention (CDC), "Covid-19 vaccines for moderately to severely immunocompromised people." `https://www.cdc.gov/coronavirus/2019-ncov/vaccines/recommendations/immuno.html`, 2021.

[75] H. E. Randolph and L. B. Barreiro, “Herd immunity: Understanding covid-19,” *Immunity*, vol. 52, no. 5, pp. 737–741, 2020.

[76] U. C. Bureau, “"tenure by household size", 2014-2018, american community survey 5-year estimates-b25009.” Web, 2018.

[77] S. Ruggles, S. Flood, R. Goeken, J. Grover, E. Meyer, J. Pacas, and M. Sobek, “Ipums usa: Version 10.0 [dataset]. minneapolis, mn: Ipums.” https://doi.org/10.18128/D010.V10.0.

[78] Springfield News Leader, “Covid19 vaccine tracker,” 2021.

[79] Centers for Disease Control and Prevention (CDC), “About variants of the virus that causes covid-19,” 2021.

[80] H. Tanaka, A. Hirayama, H. Nagai, C. Shirai, Y. Takahashi, H. Shinomiya, C. Taniguchi, and T. Ogata, “Increased transmissibility of the sars-cov-2 alpha variant in a japanese population,” *International Journal of Environmental Research and Public Health*, vol. 18, no. 15, 2021. doi: 10.3390/ijerph18157752.

[81] K. A. Brown, S. Tibebu, N. Daneman, K. Schwartz, M. Whelan, and S. Buchan, “Comparative household secondary attack rates associated with b.1.1.7, b.1.351, and p.1 sars-cov-2 variants,” *medRxiv*, 2021. doi: 10.1101/2021.06.03.21258302.

[82] T. Charmet, L. Schaeffer, R. Grant, S. Galmiche, O. Chény, C. Von Platen, A. Maurizot, A. Rogoff, F. Omar, C. David, A. Septfons, S. Cauchemez, A. Gaymard, B. Lina, L. H. Lefrancois, V. Enouf, S. van der Werf, A. Mailles, D. Levy-Bruhl, F. Carrat, and A. Fontanet, “Impact of original, b.1.1.7, and b.1.351/p.1 sars-cov-2 lineages on vaccine effectiveness of two doses of covid-19 mrna vaccines: Results from a nationwide case-control study in france,” *The Lancet Regional Health - Europe*, vol. 8, 2021. doi:https://doi.org/10.1016/j.lanepe.2021.100171.

[83] J. Lopez Bernal, N. Andrews, C. Gower, E. Gallagher, R. Simmons, S. Thelwall, J. Stowe, E. Tessier, N. Groves, G. Dabrera, R. Myers, C. N. Campbell, G. Amirthalingam, M. Edmunds, M. Zambon, K. E. Brown, S. Hopkins, M. Chand, and M. Ramsay, “Effectiveness of covid-19 vaccines against the b.1.617.2 (delta) variant,” *New England Journal of Medicine*, vol. 385, no. 7, pp. 585–594, 2021.

[84] R. M. Viner, O. T. Mytton, C. Bonell, G. J. Melendez-Torres, J. Ward, L. Hudson, C. Waddington, J. Thomas, S. Russell, F. van der Klis, A. Koirala, S. Ladhani, J. Panovska-Griffiths, N. G. Davies, R. Booy, and R. M. Eggo, "Susceptibility to SARS-CoV-2 Infection Among Children and Adolescents Compared With Adults: A Systematic Review and Meta-analysis," *JAMA Pediatrics*, vol. 175, pp. 143–156, 02 2021.

[85] S. Hu, W. Wang, Y. Wang, M. Litvinova, K. Luo, L. Ren, Q. Sun, X. Chen, G. Zeng, J. Li, L. Liang, Z. Deng, W. Zheng, M. Li, H. Yang, J. Guo, K. Wang, X. Chen, Z. Liu, and H. Yu, "Infectivity, susceptibility, and risk factors associated with sars-cov-2 transmission under intensive contact tracing in hunan, china," *Nature Communications*, vol. 12, 03 2021. doi: 10.1038/s41467-021-21710-6.

[86] N. G. Davies, P. Klepac, Y. Liu, K. Prem, M. Jit, and R. M. Eggo, "Age-dependent effects in the transmission and control of COVID-19 epidemics," *Nature Medicine*, vol. 26, pp. 1205–1211, Aug. 2020.

[87] I. Dattner, Y. Goldberg, G. Katriel, R. Yaari, N. Gal, Y. Miron, A. Ziv, R. Sheffer, Y. Hamo, and A. Huppert, "The role of children in the spread of covid-19: Using household data from bnei brak, israel, to estimate the relative susceptibility and infectivity of children," *PLOS Computational Biology*, vol. 17, pp. 1–19, 02 2021.

[88] M. S. Lau, B. Grenfell, K. Nelson, and B. Lopman, "Characterizing super-spreading events and age-specific infectivity of covid-19 transmission in georgia, usa," *Proceedings of the National Academy of Sciences*, vol. 117, no. 36, pp. 22430–22435, 2020.

[89] K. Prem, A. R. Cook, and M. Jit, "Projecting social contact matrices in 152 countries using contact surveys and demographic data," *PLOS Computational Biology*, vol. 13, Sept. 2017. doi: 10.1371/journal.pcbi.1005697.

[90] F. Xia, X. Yang, R. A. Cheke, and Y. Xiao, "Quantifying competitive advantages of mutant strains in a population involving importation and mass vaccination rollout," *Infectious Disease Modelling*, vol. 6, pp. 988–996, 2021.

[91] I. Locatelli, B. Trächsel, and V. Rousson, "Estimating the basic reproduction number for COVID-19 in western europe," *PLOS ONE*, vol. 16, no. 3, 2021. doi: 10.1371/journal.pone.0248731.

[92] J. Hall, R. Harris, A. Zaidi, S. Woodhall, G. Dabrera, and J. Dunbar, "Hosted—england's household transmission evaluation dataset: preliminary findings from a novel passive surveillance system of covid-19," *International Journal of Epidemiology*, vol. 50, 2021. doi: 10.1093/ije/dyab057.

[93] S. Haroon, J. Chandan, J. Middleton, and K. Cheng, "Covid-19: Breaking the chain of household transmission," *BMJ*, vol. 370, 2020. doi: 10.1136/bmj.m3181.